Method for calculating the global structure of (singular) spacetimes

Peter Hübner
Max-Planck-Gesellschaft Arbeitsgruppe Gravitationstheorie, an der Universität Jena, Max-Wien-Platz 1, D-07743 Jena, Germany
(Received 14 September 1994)

A formalism and its numerical implementation is presented which allows one to calculate quantities determining the spacetime structure in the large directly. This is achieved by conformal techniques by which null infinity ($\mathcal{I}^+$) and future timelike infinity (i^+) are mapped to grid points on the numerical grid. The determination of the causal structure of singularities, the localization of event horizons, the extraction of radiation, and the avoidance of unphysical reflections at the outer boundary of the grid, are demonstrated with calculations of spherically symmetric models with a scalar field as matter and radiation model.

PACS number(s): 04.20.Dw, 04.20.Ha, 04.25.Dm

I. INTRODUCTION

A. General framework

From the singularity theorems of Hawking and Penrose it is known that the appearance of singularities in general relativity is an unavoidable feature for "strong" initial data [1]. Conversely, it has been proven recently that for small initial data the future of the initial value hypersurface looks in the large in a certain sense like the future of flat space data [2–4]. Unfortunately, it has turned out to be extremely difficult to obtain reasonable conjectures, not to mention the proofs, about the properties of a spacetime given by an initial value problem, as illustrated, for example, by the history of the cosmic censorship hypothesis.

Getting an overview for the phenomena appearing and making reasonable conjectures is an area in which numerical relatively can contribute a lot to and actually already has, most impressively illustrated by the discovery of the echoing property by Choptuik [5]. But most of the codes used so far are designed to analyze local behavior. Statements about the behavior in the large ("global issues") are obtained by assuming that the extension of the grid used approximates an infinite grid well enough. This way it is very difficult, if not impossible, to get a reliable error estimate and to decide what is sufficiently far.

But what global issues are of interest and why are they interesting?

First, there are questions related to cosmic censorship, especially the location and penetration of an event horizon, which is the boundary of the region of spacetime from where no null geodesic reaches null infinity. In a recent review article [6] about cosmic censorship Clarke writes about the location of event horizons: "In terms of numerical simulations, this means that it is essential to perform the simulations in the compactified picture in which $\mathcal{I}^+$ is represented explicitly."

Secondly, there is the whole topic of gravitational radiation on asymptotically flat spacetimes. Because of the gauge freedom and the nonlinearity of the theory the classification of radiation as ingoing and outgoing is a difficult issue. In- and outgoing gravitational waves are defined with respect to null infinity only. The related difficulties in extracting gravitational waves from the grid at finite distances and the problem with the avoidance of an unphysical reflection on the outer boundary of the grid are well known and have been a topic for research for a long time. In most methods developed so far the error made consists of the error from reading off at finite distances and the discretization error.

In this paper I will present the numerical implementation of a formalism allowing one to calculate a "compactified" spacetime including $\mathcal{I}^+$ and i^+. The solution of the problems concerning radiation is trivial by construction as will be seen. The only errors which appear are caused by the discretization error of the numerical partial differential equation solver. These errors can be estimated and controlled by grid extrapolation techniques (e.g., Richardson extrapolation). Although the calculations have been done under the assumption of spherical symmetry with a scalar field as model for radiation the simplicity and exactness of radiation extraction hold for arbitrary symmetry assumptions.

Furthermore, due to the spherical symmetry a special coordinate gauge could be found allowing one to cover the complete domain of dependence of the initial hypersurface and to calculate the causal structure of a singularity. The location of the event horizon is straightforward. The formalism is based on conformal techniques developed by Penrose to describe asymptotically flat spacetimes. By a rescaling $g_{ab} = \Omega^2 \tilde{g}_{ab}$ the physical spacetime $(\tilde{M}, \tilde{g}_{ab})$ is mapped to an unphysical spacetime (M, g_{ab}, Ω) with boundary $\mathcal{I}$. The boundary represents null infinity. M is

 ©1996 The American Physical Society

a "compactified"[1] version of $\tilde{M}$. Gravitational radiation is the value of certain components of the Weyl spinor on that boundary. In the originally suggested form the formalism is not suited to describe initial value problems. Friedrich has modified it to describe initial value problems—one has to solve a set of evolution equations for the unphysical spacetime (M, g_{ab}, Ω). The rescaling factor Ω acts like an artificial matter field for the Einstein equations. Subsection II B reviews the equations for the unphysical spacetime. Winicour and Gomez have developed an approach which uses Bondi's ideas for describing gravitational radiation: Outgoing null cones, with the area distance and the direction angle as coordinates on it, are compactified to represent future null infinity by grid points. Their method gives simpler equations but has certain disadvantages: The existence of smooth outgoing null cones is essential. Null caustics, which are caused, e.g., by gravitational lensing effects, must not appear. Furthermore their evolution scheme cannot penetrate event horizons.[2] The extraction of some radiative quantities like the Bondi mass is complicated slightly as the Weyl spinor is not a variable of the system—the determination of gravitational radiation requires one to calculate numerically derivatives on $\mathcal{I}$. Their formalism solves a characteristic initial value problem; the formalism presented here solves a "normal," spacelike initial value problem in unphysical spacetime.

B. Description of asymptotically flat spacetimes with conformal techniques

Shortly after Bondi *et al.* [7] proved that gravitational radiation is not a gauge effect Penrose suggested a coordinate independent way to characterize asymptotically flat spaces and gravitational radiation. A thorough discussion of the ideas and the interpretation can be found at various places in the literature, e.g., [8,9]. The definitions of asymptotical flatness given in the literature differ slightly. The following will be used here.

Definition 1. A spacetime $(\tilde{M}, \tilde{g}_{ab})$ is called *asymptotically flat* if there is another "unphysical" spacetime (M, g_{ab}) with boundary $\mathcal{I}$ and a smooth embedding by which $\tilde{M}$ can be identified with $M - \mathcal{I}$ such that (1) there is a smooth function Ω on M with

$$\Omega|_{\tilde{M}} > 0 \text{ and } g_{ab}|_{\tilde{M}} = \Omega^2 \tilde{g}_{ab} ,$$

(2) on $\mathcal{I}$,

$$\Omega = 0 \text{ and } \nabla_a \Omega \neq 0 ,$$

and (3) each null geodesic in $(\tilde{M}, \tilde{g}_{ab})$ acquires a past and a future end point on $\mathcal{I}$.

Because of item (3) null geodesically incomplete spacetimes like Schwarzschild are not asymptotically flat. The next definition includes spacetimes which have only an asymptotically flat part like Schwarzschild.

Definition 2. A spacetime is called *weakly asymptotically flat* if definition 1 with the exception of item (3) is satisfied.

Definitions 1 and 2 classify spacetimes; they do not require that the Einstein equation is fulfilled. For a physical problem one would like to give "asymptotically flat data" and evolve them according to the Einstein equation.

Nevertheless the geometrically description was extremely helpful in analyzing asymptotically flat spacetimes and it has been successfully used as a guideline to construct a formalism for analyzing initial value problems. This method has been developed and applied to various matter sources by Friedrich [3,10–15] and myself [4].

The idea is to choose a spacetime initial value surface in the unphysical spacetime (M, g_{ab}) and to evolve it. For Minkowski space the unphysical spacetime (M, g_{ab}) can be smoothly extended with three points, future (i^+) and past (i^-) timelike infinity, the end and the starting point of all timelike geodesics of $(\tilde{M}, \tilde{g}_{ab})$, respectively, and spacelike infinity (i^0), the end point of all spacelike geodesics of $(\tilde{M}, \tilde{g}_{ab})$. The point i^0 divides $\mathcal{I}$ into two disjunct parts, future $(\mathcal{I}^+)$ and past $(\mathcal{I}^-)$ null infinity. It is well known and has been discussed elsewhere that there are unsolved problems in smoothly extending a "normal" Cauchy hypersurface of $\tilde{M}$ to i^0 if the spacetime has nonvanishing Arnowitt-Deser-Misner (ADM) mass. Certain curvature quantities blow up at i^0, reflecting the noninvariance of the mass under rescalings.

By choosing a spacelike (with respect to g_{ab}) hypersurface S not intersecting i^0 but $\mathcal{I}^+$ $(\mathcal{I}^-)$ we avoid the problems with i^0. S is called a hyperboloidal hypersurface—the corresponding initial value problem is called a hyperboloidal initial value problem.

The well posedness of the hyperboloidal initial value problem for general relativistic scalar fields has been discussed in [4]. There, a precise definition of a hyperboloidal initial value problem can be found, too.

Figure 1 shows a diagram of the unphysical spacetime with an example of a hyperboloidal surface in it. In Fig. 2 the corresponding physical spacetime is shown. In both figures only one space coordinate is drawn. All points, except those on the axis and i^0, represent spheres.

The domain of dependence $D(S)$ of S will not contain the complete spacetime. The interior of S corresponds to an everywhere spacelike hypersurface in the physical spacetime which approaches a null hypersurface N asymptotically. If N is a light cone L then the domain of dependence of S is L. Therefore the hyperboloidal initial value problem is well suited to describe the future (past) of data on the spacelike hypersurface S, e.g., a stellar object and the gravitational radiation caused by its future time evolution. It is not well suited to investigate the structure near i^0.

---

[1] M is not really compact in a strict sense—in Minkowski spacetime there are three points, future and past timelike and spacelike infinity, missing. In general M cannot be smoothly extended to contain those points.

[2] Using noncompactified null cones allows one to penetrate the event horizon.

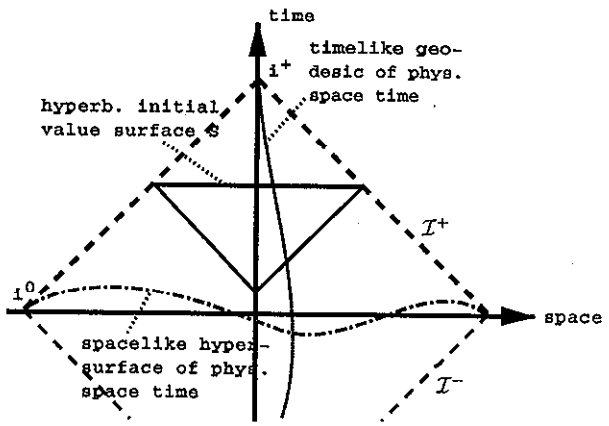

FIG. 1. Unphysical Minkowski spacetime.

Why is it advantageous to solve the initial value problem in the unphysical spacetime? The future of the data in physical spacetime $(\tilde{M}, \tilde{g}_{ab})$ is completely determined by the data on the interior of S. Since the rescaling factor Ω is known, the calculation of quantities of physical spacetime from the unphysical quantities is merely algebra. In unphysical spacetime $\mathcal{I}^+$ is on the grid. $\mathcal{I}^+$ is an ingoing null cone starting at the two-dimensional-surface in S where Ω vanishes. By extending S a little bit beyond the intersection with $\mathcal{I}$ in unphysical spacetime we do not change the physical spacetime $(\tilde{M}, \tilde{g}_{ab})$. But with a finite number of gridpoints and thus a finite computation time the whole future of the initial hypersurface is covered. And since $\mathcal{I}^+$ is an ingoing null line the values at $\tilde{M}$ and $\mathcal{I}^+$, describing the physics, do not depend on the values at the outer boundary of the extended S. The numerical dependence on the outer boundary must converge to 0.

Future null infinity, $\mathcal{I}^+$, which can be found by searching for the $\Omega = 0$ contour, is on the grid. By an appropriate choice of gauge it can even be arranged that the position of $\mathcal{I}$ on the grid is known by analytical considerations. In the worst case, one has to interpolate between neighboring grid points to find the radiation emitted. In the case of gravitational radiation, it is given by certain components of the Weyl tensor, which are variables in the system of equations for the unphysical spacetime.

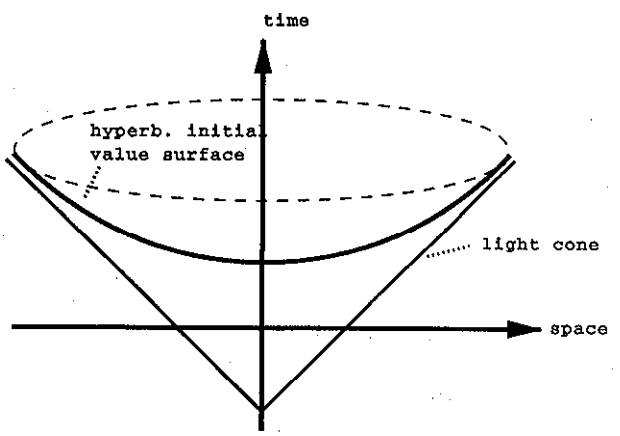

FIG. 2. Physical Minkowski spacetime.

II. THE MODEL AND THE SYSTEM OF EQUATIONS IN UNPHYSICAL SPACETIME

A. The model

The choice of the model is always a compromise between generality and manageability. For this work it was necessary to have some model for radiation to demonstrate the simplicity of the radiation extraction in the formalism. On the other side the spacetime symmetry should be as high as possible to reduce the demand for computational resources and to simplify coordinate choice related questions.

The spacetime is assumed to be spherically symmetric, the radiational degree of freedom is modeled by a conformally invariant scalar field. The equations are

$$\tilde{\Box}\tilde{\phi} - \frac{\tilde{R}}{6}\tilde{\phi} = 0 \,, \tag{1a}$$

$$(1 - \tfrac{1}{4}\kappa\tilde{\phi}^2)\tilde{R}_{ab} = [\kappa(\tilde{\nabla}_a\tilde{\phi})(\tilde{\nabla}_b\tilde{\phi}) - \tfrac{1}{2}\kappa\tilde{\phi}\tilde{\nabla}_a\tilde{\nabla}_b\tilde{\phi} - \tfrac{1}{4}\kappa\tilde{g}_{ab}(\tilde{\nabla}^c\tilde{\phi})(\tilde{\nabla}_c\tilde{\phi})] \,, \tag{1b}$$

where the second is equivalent to $\tilde{G}_{ab} = \kappa\tilde{T}_{ab}$ with

$$\tilde{T}_{ab} = (\tilde{\nabla}_a\tilde{\phi})(\tilde{\nabla}_b\tilde{\phi}) - \tfrac{1}{2}\tilde{\phi}\tilde{\nabla}_a\tilde{\nabla}_b\tilde{\phi} + \tfrac{1}{4}\tilde{\phi}^2\tilde{R}_{ab} - \tfrac{1}{4}\tilde{g}_{ab}[(\tilde{\nabla}^c\tilde{\phi})(\tilde{\nabla}_c\tilde{\phi}) + \tfrac{1}{6}\tilde{\phi}^2\tilde{R}] \,. \tag{1c}$$

The notation used is explained in Appendix A.

The form invariance of (1a) under the rescalings $g_{ab} = \Omega^2\tilde{g}_{ab}$ and $\phi = \Omega^{-1}\tilde{\phi}$ was the reason for not choosing the massless Klein-Gordon scalar field with its simpler equations in physical spacetime. In [4] it has been shown that the initial value problems for these matter models are equivalent for practical purposes.

B. The equations for unphysical spacetime

In [4] it has been argued that the Einstein equation, if simply translated to the unphysical spacetime, becomes "singular" on $\mathcal{I}$ and thus is not suitable to calculate the unphysical spacetime (M, g_{ab}). For a derivation of regular equations for the unphysical spacetime the reader is referred to [4]; here only the final first order set of equations is given.

In this first order system, the variables are the components of the frame $e_{\underline{k}}{}^a$ with respect to the coordinates x^μ, $e_{\underline{k}}{}^\mu$, the frame components $\gamma^{\underline{m}}{}_{\underline{jk}}$ of the Ricci rotation coefficients $\gamma^a{}_{\underline{jk}}$, certain combinations of the components of the tracefree part $\hat{R}_{ab}$ of the Ricci tensor and the regularized Weyl tensor $d_{abc}{}^d := \Omega^{-1}C_{abc}{}^d$, the conformal factor Ω, the frame components $\Omega_{\underline{i}}$ of its gradient Ω_a, the trace of its second derivative ω, the conformal scalar field ϕ, the frame components $\phi_{\underline{i}}$ of its gradient ϕ_a and combinations of its second derivatives $\phi_{ab} =: \hat{\phi}_{ab} + \frac{1}{4}g_{ab}\phi_c{}^c$. The first order system, written in abstract index notation is[3]

[3]The symbol $\mathcal{N}$ stands for null quantity; the first index refers to the quantity for which an equation will be formed by setting the tensor $\mathcal{N}$ equal to 0.

$$\mathcal{N}_{\mathbf{e}}{}^{a}{}_{bc} := T^{a}{}_{bc} = 0 \,, \tag{2a}$$

$$\mathcal{N}_{\gamma abc}{}^{d} := R_{\mathbf{diff}abc}{}^{d} - R_{\mathbf{alg}abc}{}^{d} = 0 \,, \tag{2b}$$

$$\begin{aligned}\mathcal{N}_{\mathbf{R}abc} := {} & \nabla_{[a}\hat{R}_{b]c} + \tfrac{1}{12}(\nabla_{[a}R)g_{b]c} - \Omega_d d_{abc}{}^{d} + \Omega m_{abc} \\ & - \tfrac{2}{3}\Omega m_{[a|d|}{}^{d} g_{b]c} \\ & = 0 \,,\end{aligned} \tag{2c}$$

$$\mathcal{N}_{\mathbf{d}abc} := \nabla_d d_{abc}{}^{d} - m_{abc} + \tfrac{2}{3} m_{[a|d|}{}^{d} g_{b]c} = 0 \,, \tag{2d}$$

$$\mathcal{N}_{\mathbf{\Omega}a} := \nabla_a \Omega - \Omega_a = 0 \,, \tag{2e}$$

$$\mathcal{N}_{\mathbf{D\Omega}ab} := \nabla_a \Omega_b + \tfrac{1}{2}\Omega\hat{R}_{ab} - \omega g_{ab} - \tfrac{1}{2}\Omega^3 T_{ab} = 0 \,, \tag{2f}$$

$$\begin{aligned}\mathcal{N}_{\omega ab} := {} & \nabla_a \omega + \tfrac{1}{2}\hat{R}_{ab}\Omega^b + \tfrac{1}{12}R\Omega_a + \tfrac{1}{24}\Omega\nabla_a R \\ & - \tfrac{1}{2}\Omega^2 T_{ab}\Omega^b \\ & = 0 \,,\end{aligned} \tag{2g}$$

$$\mathcal{N}_{\phi a} := \nabla_a \phi - \phi_a = 0 \,, \tag{2h}$$

$$\mathcal{N}_{\mathbf{D}\phi ab} := \nabla_a \phi_b - \hat{\phi}_{ab} - \tfrac{1}{4}\phi_c{}^{c} g_{ab} = 0 \,, \tag{2i}$$

$$\mathcal{N}_{\Box\phi} := \phi_a{}^{a} - \frac{R}{6}\phi = 0 \,, \tag{2j}$$

$$\begin{aligned}\mathcal{N}_{\mathbf{DD}\phi abc} := {} & \nabla_{[a}\hat{\phi}_{b]c} + \tfrac{1}{6}(\phi\nabla_{[a}R + R\phi_{[a})g_{b]c} \\ & - \tfrac{1}{2}R_{\mathbf{alg}abc}{}^{d}\phi_d = 0 \,,\end{aligned} \tag{2k}$$

$$\mathcal{N}_{\mathbf{D}\Box\phi a} := \nabla_a \phi_b{}^{b} - \tfrac{1}{6}(\phi\nabla_a R + R\phi_a) = 0 \,, \tag{2l}$$

where $T^{a}{}_{bc}$ is the torsion whose components are given by

$$T^{\underline{i}}{}_{\underline{jk}} = [e_{\underline{j}}(e_{\underline{k}}{}^{\mu}) - e_{\underline{k}}(e_{\underline{j}}{}^{\mu})]e^{\underline{i}}{}_{\mu} + \gamma^{\underline{i}}{}_{\underline{jk}} - \gamma^{\underline{i}}_{\underline{kj}} \,,$$

the tensor $R_{\mathbf{alg}abc}{}^{d}$ is an abbreviation for

$$R_{\mathbf{alg}abcd} = \Omega d_{abcd} + g_{c[a}\hat{R}_{b]d} - g_{d[a}\hat{R}_{b]c} + \tfrac{1}{6}g_{c[a}g_{b]d}R \,, \tag{3}$$

the algebraic decomposition of a tensor with the same index symmetry properties as the Riemann tensor (therefore the index **alg**), $R_{\mathbf{diff}abc}{}^{d}$ has the components

$$\begin{aligned}R_{\mathbf{diff}\underline{ijk}}{}^{\underline{l}} = {} & e_{\underline{j}}(\gamma^{\underline{l}}{}_{\underline{ik}}) - e_{\underline{i}}(\gamma^{\underline{l}}{}_{\underline{jk}}) - \gamma^{\underline{l}}{}_{\underline{im}}\gamma^{\underline{m}}{}_{\underline{jk}} + \gamma^{\underline{l}}{}_{\underline{jm}}\gamma^{\underline{m}}{}_{\underline{ik}} \\ & + \gamma^{\underline{m}}{}_{\underline{ij}}\gamma^{\underline{l}}{}_{\underline{mk}} + \gamma^{\underline{m}}{}_{\underline{ji}}\gamma^{\underline{l}}{}_{\underline{mk}} - \gamma^{\underline{l}}{}_{\underline{mk}}T^{\underline{m}}{}_{\underline{ji}} \,,\end{aligned}$$

which is the curvature expressed as differential of the connection (therefore the index **diff**), the "energy momentum tensor" in unphysical spacetime is

$$T_{ab} = \phi_a\phi_b - \tfrac{1}{2}\phi\phi_{ab} + \tfrac{1}{4}\phi^2 R_{ab} - \tfrac{1}{4}g_{ab}\left(\phi_c\phi^c + \tfrac{1}{6}\phi^2 R\right)$$

and

$$\begin{aligned}m_{abc} = \frac{1}{1-\frac{1}{4}\Omega^2\phi^2}\Bigg(& \Omega[\tfrac{3}{2}\phi_{[a}\phi_{b]c} - \tfrac{1}{2}g_{c[a}\phi_{b]d}\phi^d + \tfrac{1}{4}\phi\Omega d_{abc}{}^{d}\phi_d + \tfrac{1}{4}\phi g_{c[a}\hat{R}_{b]}{}^{d}\phi_d - \tfrac{3}{4}\phi\phi_{[a}\hat{R}_{b]c} \\ & - \tfrac{1}{12}\phi\phi_{[a}g_{b]c}R + \tfrac{1}{4}\Omega\phi^2 d_{abc}{}^{d}\Omega_d] - 3\Omega_{[a}\left[\phi_{b]}\phi_c - \tfrac{1}{2}\phi\phi_{b]c} + \tfrac{1}{4}\phi^2\hat{R}_{b]c} + \tfrac{1}{36}\phi^2 g_{b]c}R - \tfrac{1}{3}g_{b]c}\phi^d\phi_d\right] \\ & + \Omega^d g_{c[a}\left[\phi_{b]}\phi_d - \tfrac{1}{2}\phi\phi_{b]d} + \tfrac{1}{4}\phi^2\hat{R}_{b]d}\right]\Bigg) \,.\end{aligned}$$

Unfortunately the terms introduced into the system by the scalar field, T_{ab} and m_{abc}, complicate the equations a lot due to the form of the energy momentum tensor for the conformally invariant scalar field.

Furthermore there is an additional equation,

$$\Omega^2 R + 6\Omega\nabla^a\nabla_a\Omega - 12(\nabla^a\Omega)(\nabla_a\Omega) = 0 \,, \tag{4}$$

which must be satisfied at one point to be automatically satisfied everywhere. If we fulfill Eq. (4) at one point the function $R(t,r)$ can be given freely. It determines the gauge freedom in the conformal factor Ω to a certain extent. If (M, g_{ab}, Ω) is a solution of the unphysical equations so is $(M, \theta^2 g_{ab}, \theta\Omega)$ for $\theta > 0$. In all the calculations, R has been set to 6, the value obtained if the compactification for Minkowski space given in [16] is used. The program code does allow one to specify $R(t,r)$. The conformal gauge freedom has been discussed in more detail in [4].

C. Simplifications by the spherical symmetry and the remaining gauge freedom

The first order system (2) is an underdetermined system. To make it complete the coordinate and frame gauge freedom must be fixed. This will be done in this section. Furthermore the number of variables will be reduced significantly by making use of the spherical symmetry.

A spacetime is said to be spherically symmetric if it possesses an isometry group I which contains a subgroup R which is isomorphic to the three-dimensional group SO(3) and whose orbits are orientable submanifolds of dimension < 3. The orbits of R are either (fixed) points or spheres $\mathbb{S}^2$. The fixed points form at most two timelike geodesics as can be seen by symmetry arguments. It is assumed that the initial hypersurface intersects with at

least one line of fixed points, i.e., there is a (regular) center on the initial hypersurface.

But no attempt was made to use every simplification spherical symmetry provides for the following reason: It is well known that Einstein's equations can be reduced to two ordinary differential equations (constraints) [17] plus matter equations in spherical symmetry. The circumstance that no equation with a time derivative for the geometry variables must be solved can be viewed as expressing the lack of gravitational radiation in spherical symmetry. I have not made any attempt to incorporate this kind of simplification into the system for the unphysical spacetime, since the calculations are supposed to be a playground for testing and learning about the advantages and disadvantages of the formalism for a later application to models with less symmetry.

In the gauge used the system is symmetric hyperbolic and the coordinates cover the whole domain of dependence of the initial hypersurface. It is not known to the author how to construct such a coordinate system in less symmetric spacetimes. The very nice feature of semilinearity is certainly an artifact of spherical symmetry.

1. Gaussian gauge

In the analytical analysis of the initial value problem with scalar fields as source terms, a Gaussian gauge was used [4]. This gauge gives a symmetric hyperbolic subsidiary system of equations. If the energy momentum tensor fulfills certain conditions, the coordinate system will break down because of the formation of caustics [16]. Whether the region of the unphysical spacetime representing the physical spacetime can be covered by the use of a Gaussian gauge in unphysical spacetime is not obvious since the conformal rescaling factor Ω acts as a kind of artificial energy-momentum source in unphysical spacetime. By numerical calculations it was straightforward to show that even in unphysical spacetime a Gaussian gauge will lead to caustics [18], and is thus inappropriate to analyze the strong field regime. The system of equations is very similar to the one obtained in "double null" coordinates except that it is not semilinear. It will not be discussed any further.

2. "Double null" gauge

The construction of the coordinate system and the frame are described starting from an initial hypersurface. The remarks about the differentiability class of the objects assume that the construction is done with respect to a given C^∞ manifold (for a definition see [16, Sec. 1.1.1]). The investigation of the differentiability is necessary to ensure that a discontinuity of a value or even a singular value of a variable at the center is not caused by lacking smoothness of the coordinates. The gauge realized in this way turns out to be an obvious adherent of double null coordinates. Assume we are given a spacelike C^∞ hypersurface S with $t = t_0$. This hypersurface is factored by the orbits of the group. By the geodesics running from the center in the different directions the angle coordinate (ϑ, φ) with line element $d\vartheta^2 + \sin^2\vartheta\, d\varphi$ on the unit sphere are defined on all orbits. By isotropy the geodesics are perpendicular to the orbits. The orbits are labeled by a monotonically increasing coordinate r, defined to be 0 at the center. Auxiliary coordinates (u, v) are defined by $u := (t_0 - r)/2$ and $v := (t_0 + r)/2$. Set (u, ϑ, φ)=const along the future directed, outgoing null lines, (v, ϑ, φ) =const along the future directed, ingoing null line. On passing through the center set $u = v$. Because of the spherical symmetry there cannot be any null caustic; a break down of the coordinates is aligned with a spacetime singularity. By (u, v) a timelike coordinate

$$t = u + v \tag{5}$$

and a spacelike coordinate

$$r = v - u \tag{6}$$

are defined everywhere in the domain of dependence of S. An orthonormal frame field $(e_{\underline{0}}{}^a, e_{\underline{1}}{}^a, e_{\underline{2}}{}^a, e_{\underline{3}}{}^a)$ is defined except in the center (polar coordinate singularity) by normalizing the orthogonal vector fields $(\partial_t{}^a, \partial_r{}^a, \partial_\vartheta{}^a, \partial_\varphi{}^a)$.

As shown in [18] the t =const hypersurfaces are at least C^3 and hence sufficiently smooth. The proof proceeds in two steps: first it is shown that there is a C^∞ transformation to radar coordinates; secondly a theorem by Proff [19, theorem 1.2.4] about radar coordinates completes the proof.

In this coordinate system the following relations hold: The frame-coordinate matrix is diagonal,

$$(e_{\underline{0}}{}^\mu, e_{\underline{1}}{}^\mu, e_{\underline{2}}{}^\mu, e_{\underline{3}}{}^\mu) = \begin{pmatrix} e_{\underline{0}}{}^0(t,r) & 0 & 0 & 0 \\ 0 & e_{\underline{1}}{}^1(t,r) & 0 & 0 \\ 0 & 0 & e_{\underline{2}}{}^2(t,r) & 0 \\ 0 & 0 & 0 & e_{\underline{2}}{}^2(t,r)/\sin\vartheta \end{pmatrix} \tag{7}$$

and

$$e_{\underline{0}}{}^0(t,r) = e_{\underline{1}}{}^1(t,r)\ . \tag{8}$$

All Ricci rotation coefficients except

$$\gamma^{\underline{0}}{}_{\underline{01}}(t,r),\quad \gamma^{\underline{0}}{}_{\underline{11}}(t,r)\ ,$$

$$\gamma^{\underline{0}}{}_{\underline{22}}(t,r),\quad \gamma^{\underline{0}}{}_{\underline{33}}(t,r) = \gamma^{\underline{0}}{}_{\underline{22}}(t,r)\ ,$$

$$\gamma^{\underline{1}}{}_{\underline{22}}(t,r),\quad \gamma^{\underline{1}}{}_{\underline{33}}(t,r) = \gamma^{\underline{1}}{}_{\underline{22}}(t,r),\quad \gamma^{\underline{2}}{}_{\underline{33}} = -\frac{\cos\vartheta}{\sin\vartheta} e_{\underline{2}}{}^2 \tag{9}$$

vanish.

Scalars invariant under rotations are functions of (t, r) only; rotationally invariant vectors V^a are of the form

$$V^{\underline{i}} = \begin{pmatrix} V^{\underline{0}}(t,r) \\ V^{\underline{1}}(t,r) \\ 0 \\ 0 \end{pmatrix}\ , \tag{10}$$

and symmetric covariant two-tensors S_{ab}, e.g., the Ricci tensor R_{ab}, invariant under rotations, look like

$$S_{\underline{\mu\nu}} = \begin{pmatrix} S_{\underline{00}}(t,r) & S_{\underline{01}}(t,r) & 0 & 0 \\ S_{\underline{01}}(t,r) & S_{\underline{11}}(t,r) & 0 & 0 \\ 0 & 0 & S_{\underline{22}}(t,r) & 0 \\ 0 & 0 & 0 & S_{\underline{22}}(t,r) \end{pmatrix} . \quad (11)$$

This follows from the assumptions about the symmetry. All components of $d_{abc}{}^{d}$ are either zero or proportional to $d_{\underline{101}}{}^{\underline{0}}$.

3. The resulting system

Due to the complicated form of the matter terms the set of equations is very lengthy. The equations are given in Appendix B; they are derived from system (2) and

$$\partial_r \left(\frac{-\mathcal{N}_{\mathrm{e}}{}^{\underline{1}}{}_{\underline{01}}}{e_{\underline{1}}{}^{\underline{1}}} \right) - \partial_t \left(\frac{\mathcal{N}_{\mathrm{e}}{}^{\underline{0}}{}_{\underline{01}}}{e_{\underline{1}}{}^{\underline{1}}} \right) = 0 .$$

The system (2) has some remarkable features which should be mentioned. First it is semilinear. Secondly every equation has one of the following forms:

$$\partial_u \mathcal{U} = b_{\mathcal{U}}(\mathcal{U}, \mathcal{V}, \mathcal{T}) ,$$

$$\partial_v \mathcal{V} = b_{\mathcal{V}}(\mathcal{U}, \mathcal{V}, \mathcal{T}) ,$$

$$\partial_t \mathcal{T} = b_{\mathcal{T}}(\mathcal{U}, \mathcal{V}, \mathcal{T}) ,$$

where $\mathcal{U}$, $\mathcal{V}$, and $\mathcal{T}$ are variables propagating along u, v, and t. $\mathcal{U}$ stands for $\gamma 3$, $\widehat{R1}$, and $\widehat{\phi 1}$, $\mathcal{V}$ for $\gamma 3$, $\widehat{R3}$, and $\widehat{\phi 3}$, $\mathcal{T}$ for $e_{\underline{0}}{}^{0}, e, \gamma 2, \gamma, \widehat{R2}, \Omega, \Omega_{\underline{0}}, \Omega_{\underline{1}}, \phi, \phi_{\underline{0}}, \phi_{\underline{1}}$, and $d_{\underline{101}}{}^{\underline{0}}$. For every $\mathcal{T}$ there also exists a constraint:

$$\partial_r \mathcal{T} = c_{\mathcal{T}}(\mathcal{U}, \mathcal{V}, \mathcal{T}) .$$

There are no constraints for the $\mathcal{U}$ and $\mathcal{V}$.

4. The regularity conditions

Polar coordinates cause regularity conditions in the center, in physical spacetime as well as in unphysical spacetime. For the variables in the system (B3) those conditions are given in Appendix B 3. They express that locally the center behaves like Minkowski space, and indicate how a wave hitting the $r = 0$ (inner) boundary is reflected there (passes through the center). The regularity conditions at the inner boundary are the part of the code that would exchange if a spacetime with a throat were calculated. But in unphysical spacetime there are also necessary conditions for the regularity at $\mathcal{I}$, expressing an appropriate falloff in physical spacetime and therefore reflecting asymptotical flatness.

It is not known whether those conditions are also sufficient for regularity on $\mathcal{I}$ in the general case. The answer to this requires the investigation of the constraints on a given hypersurface. For the case that a neighborhood of $\mathcal{I}$ is free of matter and for a special choice of a hypersurface (for technical reasons) it has been shown that the necessary conditions are also sufficient [20]. In the calculations presented here those conditions are fulfilled. There are as many regularity conditions (at the center and at $\mathcal{I}$) as there are variables $\mathcal{T}$.

III. THE NUMERICAL METHOD

In this section the numerical methods used will be described shortly and the reasons given for choosing those methods.

A. The initial value solver

There are 12 constraints and 12 regularity conditions to be solved. The free functions in the constraints are the six variables $\mathcal{U}$ and $\mathcal{V}$. But giving those makes the interpretation of a parameter study difficult. $\mathcal{U}$ and $\mathcal{V}$ represent higher derivatives of the primary quantities, the metric g_{ab}, the rescaling factor Ω fixing the relation between physical and unphysical spacetime, and the scalar field ϕ. Furthermore the regularity conditions at $\mathcal{I}$ are easier to handle if it is known where Ω vanishes. A straightforward way to realize this is to give Ω on the initial slice.

In the code $e_{\underline{1}}{}^{1}, \gamma^{\underline{0}}{}_{\underline{11}}, \gamma^{\underline{0}}{}_{\underline{22}}, \Omega, \phi$, and $\phi_{\underline{0}}$ are given as free functions (because of regularity they all must be even at the center). $e_{\underline{1}}{}^{1} = e_{\underline{0}}{}^{0}$ determines the g_{00} respectively the g_{11} component of the metric, $\gamma^{\underline{0}}{}_{\underline{11}}$ and $\gamma^{\underline{0}}{}_{\underline{22}}$ the extrinsic curvature of the initial slice in unphysical spacetime. The constraints which contain derivatives of these quantities are interpreted as algebraic conditions for the quantities on the right-hand side. To ensure the invertibility of the resulting system, including the points where $\Omega = 0$, instead of Eq. (B29) its derivative is used. A constraint for $\widehat{R1} + \widehat{R3}$ results which becomes an algebraic condition on $\Omega = 0$ if $\widehat{R1} + \widehat{R3}$ is at least C^1 [condition (B38k)]. This is a necessary condition for a regular $\mathcal{I}$.

The differential algebraic system has boundary conditions in the center and at $\Omega = 0$. As there are as many boundary conditions as variables to solve for all the initial value freedom is coded in the free functions $e_{\underline{1}}{}^{1}, \gamma^{\underline{0}}{}_{\underline{11}}, \gamma^{\underline{0}}{}_{\underline{22}}, \Omega, \phi$, and $\phi_{\underline{0}}$. The system is solved with a relaxation scheme combined with a Newton-Raphson solver derived with minor modifications from the code given in [21]. First the system is solved between $r = 0$ and $\Omega = 0$. If desired the same scheme can be used to extend the initial hypersurface beyond the intersection with $\mathcal{I}$. For this integration boundary conditions are given at $\Omega = 0$, namely the values obtained at $\Omega = 0$ when solving the constraints "inside" $\mathcal{I}$. To avoid a dependency of the values at $\mathcal{I}$ on the treatment of the outer grid boundary the initial hypersurface has to always be slightly extended beyond $\mathcal{I}$.

To improve accuracy the system is solved with different grid sizes and the results are Richardson (or Bulirsch-Stoer) [21] extrapolated to vanishing grid size. In the test cases, where an exact solution is known, the accuracy was limited by the rounding error of the inversion of the matrix in the Newton-Raphson part of the code. Typically the numerical and the exact solution differed in the last two digits for calculations with eight byte floating point numbers.

B. The time integrator

Constrained evolution schemes are known to give in general more accurate results than free evolution schemes. But there are disadvantages of constrained evolution schemes. In a constrained evolution scheme the values at a certain grid point depend on the values at many other grid points on the same time slice. Thus if one grid point becomes singular the property of being singular is spread over the time slice into regions which are not causally connected with the singular point.

In most approaches used in numerical relativity the singularity is avoided by an appropriate choice of the coordinate system, actually the necessity of singularity avoidance has become a dogma of numerical relativity [22,23]. A quite often used example for a singularity avoiding coordinate system is obtained by the radial gauge in spherically symmetric spacetimes [5,24]. This coordinate system cannot penetrate apparent horizons which are supposed to wrap around singularities by the cosmic censorship hypothesis. The very interesting region of spacetime, where the gravitational field has become strong enough to prevent light rays from expanding, is excluded from being calculated.

The double null-like coordinate system used does not avoid singularities; the coordinate lines can only end at a singularity. In this subsection it will be described how a program crash is avoided if singular points occur and how the calculation is continued in the region of spacetime which are outside the future domain of dependence of singular points. In the chosen approach the singular boundary of spacetime is represented by grid points.

1. *Inside the grid*

To avoid the spreading of the singular property out of the domain of influence of the equations it is necessary to run the scheme, at least in the very neighborhood of a singularity, with a Courant factor of 1. Different schemes have been tested [18]. The only second order schemes which could be run at a Courant factor of 1 were the second order schemes of the class S^{α}_{β} [25] with $\beta = 1/2$. A second order Law-Wendroff scheme as follows has been chosen: For the equation $\partial_t F_I = \lambda_I \partial_r f_I + b(\underline{f})$, with λ_I =const and a vector of functions, $\underline{f}$, the predictor step is

$$f^{j+1/2}_{I_{i-1/2}} = \frac{1}{2}(f^j_{I_{i-1}} + f^j_{I_i}) + \frac{\Delta t}{2\Delta r}\lambda_I (f^j_{I_i} - f^j_{I_{i-1}}) + \frac{\Delta t}{2} b\left(\frac{1}{2}(\underline{f}^j_{i-1} + \underline{f}^j_i)\right) .$$

Then the corrector step is

$$f^{j+1}_{I_i} = f^j_{I_i} + \frac{\Delta t}{\Delta r}\lambda_I (f^{j+1/2}_{I_{i+1/2}} - f^{j+1/2}_{I_{i-1/2}}) + \Delta t\, b\left(\frac{1}{2}(\underline{f}^{j+1/2}_{i-1/2} + \underline{f}^{j+1/2}_{i+1/2})\right) .$$

If λ_I were a function of $\underline{f}$, as it is the case for other coordinate choices, it would be discretized as b. The second order Lax-Wendroff scheme is used to evolve gridpoints not depending on the values at the boundary.

2. *At the boundaries*

The treatment at the outer boundary is irrelevant as long as the scheme remains stable for the following reason: The initial value surface is extended beyond the intersection with $\mathcal{I}$. Running with a Courant factor of 1 the points inside and on $\mathcal{I}$, representing the physical spacetime, do not even depend on the values at the outer boundary which has no intersection with $\mathcal{I}$. Even if the treatment of the outer boundary causes an instability it will not influence the physics, i.e., the values on $\tilde{M}$ and $\mathcal{I}$. In most runs with Courant factor 1 the grid points depending on the outer boundary have not even been calculated. For a run with a Courant factor < 1 the influence of the outer boundary treatment on the physical spacetime must converge to 0 with the same order the scheme converges. Thus as long as the treatment on the outer boundary is numerically stable the values at $\tilde{M}$ and $\mathcal{I}$ are in the limit of vanishing grid size independent of the outer boundary treatment at any physical time.

Finding a stable treatment of the center was a very difficult problem. So far I could not find a treatment which remains stable if a fourth order scheme is built from the second order Lax-Wendroff by Richardson extrapolation. Especially it was not possible to extend the grid from the gridpoints at $r = 0$ and $r = \Delta r$ to $r = -\Delta r$ and run the Lax-Wendroff scheme on the extended grid.

The solution of the stability problems at the inner boundary was to replace the values near the center after every time step by the values obtained by other methods. In the method I previously used [18] the constraints were integrated from grid point number 2 towards the center (the constraints together with the regularity conditions determine all the variables at the center). The values at grid point 1 have been obtained by interpolation. The solution did not look smooth on the innermost gridpoints for coarse grids in the very strong field regime. For very large fields (values of A beyond 1.10) this method even became unstable. Therefore another method has been developed.

In the calculations for this paper a kind of polynomial extrapolation with dissipation has been used to replace the innermost grid points. The idea is the following: Use the values at grid points 2 and higher and the regularity conditions to extrapolate towards the center by polynomial fitting and get solution I. Do the polynomial fitting again starting at grid point 3 to get solution II. Solutions I and II can now be added in such a way that the simplest grid mode with values $1, -1, 1, \ldots$ is eliminated. This adding of dissipation is necessary to ensure stability. I call this method polynomial extrapolation with dissipation.

3. The singularity catcher

Since the coordinate system does not avoid singularities some variables may become singular. Depending on the default setting of the compiler this causes a crash of the program by a floating point exception (on UNIX systems the signal SIGFPE is sent). The programming language C allows one to specify what to do in case of a certain signal. In the program used the action on SIGFPE is to flag the corresponding grid point as singular and to continue the calculation on the rest of the grid. In addition to the reception of a SIGFPE signal a grid point is flagged as singular if either the principal part, i.e., $e_{\underline{0}}{}^{0}$ or $1 - \frac{1}{4}\Omega^2\phi^2$, of the equation changes sign, i.e., the system of equations becomes singular in the sense of [4], or if the evaluation of the values according to the scheme would involve points already flagged as singular (hence called influence singularity). According to the latter reason every point whose values depend on values at singular points must be flagged singular.

A necessary condition for the stability of a scheme solving symmetric hyperbolic systems is the Courant-Friedrichs-Lewy condition. The domain of dependency of the discretized equations must be a superset of the domain of dependency of the continuous equations; the Courant factor must be ≤ 1. A Courant factor of 1 means that both domains of dependency coincide. On the other hand, every grid point depending on singular gridpoints is singular. Thus all points in the future null cone L of a singular point must be flagged singular. If the Courant factor is < 1 points outside L also. For a scheme with a Courant factor of exactly 1 at least in the very vicinity of the singularity it is possible to distinguish timelike/nullike singularities from spacelike singularities. If a line of gridpoints is numerically singular only because of an influence singularity it is a strong hint for a timelike singularity behind. Pure influence singularities appeared only due to instabilities during the tests of different treatments of the center. This is in agreement with cosmic censorship.

The dependence of the position of a singular line on the grid size has been tested intensely. In all calculated cases presented the position changed only by a negligible amount corresponding to a few grid points for calculations with about 10 000 spatial points. The dependence of the first appearance of a singularity on the Courant factor has also been tested. It only changed by a few grid points when using Courant factors significantly smaller than 1.

IV. CHECKING AGAINST EXACT SOLUTIONS AND ACCURACY ESTIMATES

A. Comparing with exact solutions

On the exact solutions given below a number of tests have been performed with grids varying from 300 to 10 000 spatial grid points and different Courant factors. For most plots a coarser grid has been used, typically with 100×100 grid points.

On the plotting grid the scheme shows the expected convergence behavior. For finer grids (2000 spatial points and more) the error is dominated by second order terms. For coarser grids fourth order terms (oscillations corresponding to high Fourier modes) dominate the error near regions with steep gradients. The error predictions by Richardson's extrapolation are in good agreement with the actual error.

As time evolution is done by a free evolution scheme the constraints are only initially satisfied [26]. But it has been checked that the violation of the constraints converges at least with second order. Convergence is partly dominated by the error in the discretization of the derivative for an evaluation of the constraints. It was not possible to use the violation of the constraints as a measure for the quality of the solution.

1. Scalar field on flat background

A scalar field on a flat background is obtained by setting $\kappa = 0$ in the evolution equations. Since the physical energy-momentum tensor $\tilde{T}_{ab}$ is tracefree the Ricci scalar $\tilde{R}$ in physical spacetime vanishes. $\tilde{\phi}$ is determined by $\tilde{\Box}\tilde{\phi} = 0$.

The corresponding solution in unphysical spacetime is $\phi = \tilde{\phi}/\Omega$. On $\tilde{M}$ the following rescaling has been used:

$$\Omega(t,r) = \frac{\pm 2}{\sqrt{\left(1+\tan^2\frac{t+r}{2}\right)\left(1+\tan^2\frac{t-r}{2}\right)}} \tag{12}$$

with an obvious choice of the sign, depending on the position relative to $\mathcal{I}$ and i^+. Scalar field pulses of the initial form

$$\phi(t_0,r) = \begin{cases} e^{-1/[1-\sigma^2(r-r_0)^2]} & \text{for } |r-r_0| < 1/\sigma\,, \\ 0 & \text{otherwise}\,, \end{cases} \tag{13}$$

with constants σ and r_0, have been chosen.

This solution is useful for testing the matter part and the geometry part of the code separately since $\kappa = 0$ decouples their evolution equations. But as most of the geometry variables are just constants this is only a first step as test for the geometry part.

2. By conformal gauge freedom deformed background

For any positive function $\vartheta(t,r)$ the spacetimes $(M, \vartheta^2 g_{ab}, \phi/\vartheta)$ and (M, g_{ab}, ϕ) correspond to the same physical spacetime if (M, g_{ab}, ϕ) is a solution of the unphysical equations. This gauge freedom can be used to obtain an unphysical representation of Minkowski spacetime where the geometry variables evolve in time and are not constant (except the Weyl tensor component $d_{\underline{101}}{}^{\underline{0}}$, which is zero for every representation of Minkowski space). For θ an ingoing wave pulse with the initial form (13) plus a constant c, such that $\theta \geq 0$ everywhere, has been chosen. ϕ has been set to 0.

This solution has been used to make the geometry vari-

ables vary in time and space and is thus a better test for the geometry part of the code than the test in the previous subsection.

3. $\phi+$ const solution

In physical spacetime $\tilde{\phi}$=const is a solution for Minkowski spacetime. If we use const$\neq 0$, $\phi = \tilde{\phi}/\Omega$ is still a solution on $\tilde{M}$ in unphysical spacetime. But this solution is no longer regular on $\mathcal{I}$ thus the calculation can be done in the interior of $\tilde{M}$ only. For the tests that poses no restriction, since in the unphysical spacetime there is nothing special in the evolution equations on $\mathcal{I}$. Since in this solution $\kappa \neq 0$ and $\phi \neq 0$ the coupling between the geometry and the matter part can be tested.

B. Error estimates and problems near the critical parameter

For the nonlinear regime two ways have been used to check the accuracy of the solution. The first is Richardson extrapolation to vanishing grid size with the resulting error estimates. The second uses the fact that the position of $\mathcal{I}$ is known and thus it is possible to compare the calculated value Ω there with the exact value 0. The error estimate for Ω by Richardson extrapolation was in all cases in agreement with that deviation.

On an approach to the critical parameter, the smallest parameter where a singularity appears, there is a dramatic loss of accuracy although on the coarse plotting grid the scheme still converges quadratically. Viewing the fine grid used for the calculations one sees that the loss of accuracy is largest around grid points 5–10, and this maxima of the error decreases linearly with the grid size, meaning that there is only quadratic convergence in a L^1 norm, but not pointwise.

For models not to close to the critical value the accuracy problem described can be cured by using more grid points. But with about 50 000 spatial grid points that brute force method reaches its limitation. Since the scheme converges quadratically in a L^1 norm only, building a higher order scheme by Richardson extrapolation did not work.

A detailed inspection of the reasons hints that this is partly a problem of numerical regularization as described in [27], pp. 13–15]. When the calculations for this paper were done there was no way known to the author to numerically regularize the Lax-Wendroff scheme.

V. CALCULATIONS

In the calculations presented the free functions defining the geometry of the initial slice are given as follows:

$$e_{\underline{1}}{}^{1} = 1 \,, \tag{14}$$

$$\gamma^{0}{}_{\underline{11}} = 0 \,, \tag{15}$$

$$\gamma^{0}{}_{\underline{22}} = 0 \,, \tag{16}$$

$$\Omega = \frac{\pm 2}{\sqrt{\left(1+\tan^2\frac{t_0+r}{2}\right)\left(1+\tan^2\frac{t_0-r}{2}\right)}} \,. \tag{17}$$

The value of the time coordinate on the initial slice t_0 is $\pi/2$. The form of Ω is an often used choice for the rescaling of Minkowski space.

For the scalar field the initial value is given by

$$\phi(r) = \begin{cases} A[1-4\sigma^2(r-r_0)^2+6\sigma^4(r-r_0)^4-4\sigma^6(r-r_0)^6+\sigma^8(r-r_0)^8] & \text{for } |r-r_0|<1/\sigma \,, \\ 0 & \text{otherwise,} \end{cases} \tag{18}$$

with $\sigma = (8/\pi)$ and $r_0 = \pi/4$. This function $\phi(r)$ is the uniquely defined C^3 function with compact support $[r_0-1/\sigma, r_0+1/\sigma]$, being a polynomial of degree 8 on the support and with maximal value A at r_0. A is the parameter to be varied. $\phi(r)$ should be at least C^3 in order to have all variables in the system at least C^1 avoiding the known problems of a Lax-Wendroff scheme at discontinuities. From the numerical viewpoint this form of the pulse is much better than a "C^∞ partition of the one" like (13), since the variation of $\phi(r)$ and its spatial derivatives is better distributed over the support.

$\phi_{\underline{0}}$ is chosen in such a way that the pulse would be purely ingoing on a flat background, which is the Einstein cylinder in unphysical space, i.e.,

$$\phi_{\underline{0}} = \phi_{\underline{1}} + \phi\frac{\cos r}{\sin r} \,, \tag{19}$$

for $r - r_0 \in]-1/\sigma, 1/\sigma[$ and 0 otherwise.

A pulse with compact support provides several advantages when checking the accuracy and interpreting the numerical solution since part of the qualitative behavior of the structure in the large is known from analytic considerations. Figure 3 shows the qualitative behavior in the large for a regular solution.

Region I is the compact support of the ingoing pulse in the linear model ($\kappa = 0$), passing through the center and then crossing $\mathcal{I}$, the thick line. Every deviation from a Schwarzschild solution in region III is caused by a pure

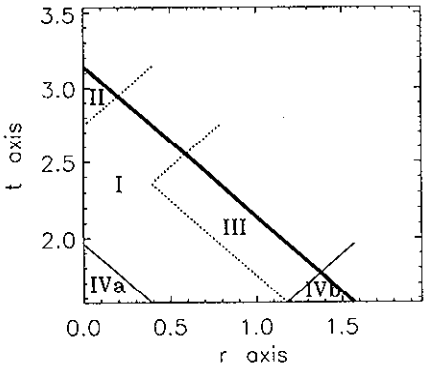

FIG. 3. Qualitative picture of the structure in the large.

backscattering effect. The deviations from flat space in region II are also a backscattering effect—the field gets caught near the center for some time. As the characteristics have slope 1, region IVa is a portion of flat space and region IVb is a portion of Schwarzschild spacetime. For stronger data the solution will become singular, before reaching the tip $(\pi, 0)$ a singularity will appear. To investigate the structure of this singularity is one of the goals of this work. In a regular spacetime timelike infinity, i^+, lies at the point $(\pi, 0)$.

A. A parameter study

With increasing parameter A more and more matter is put onto the initial slice. At some critical A^* the spacetime is expected to become singular. In this subsection the change of the global structure will be discussed and a conjecture for the critical case presented.

When interpreting the behavior with varying parameter two things have to be kept in mind. First the characteristics, null geodesics, are a common structure of all models. As the coordinates are adapted to this structure it is straightforward and well defined to compare the models. Second the area distance $\tilde{r} := \sqrt{\tilde{g}_{\theta\theta}}$ to the center in physical spacetime, expressed in unphysical variables, is

$$\tilde{r} = \frac{r}{e\Omega} .$$

Even on the initial slice e is determined as a solution of differential equations, the constraints. Depending on A the area distance of the inner and outer edge of the shell of compact support of ϕ vary (in this parameter study they monotonically grow with A). In principle it is possible, and for a better comparison with Choptuik's work desirable, to give e as a free function, but parts of the initial value solver code would have to be rewritten. But in doing so one can no longer give either Ω or components of the extrinsic curvature as free functions. The first case causes problems since the location of $S \cap \mathcal{I}$ on the grid is no longer known; in the second case it is unknown whether the necessary conditions for regularity on $\mathcal{I}$ are also sufficient.

1. The conformal factor

Figure 4 shows a contour plot of the rescaling factor Ω for modestly strong initial data corresponding to a parameter $A = 0.25$. That is well below the critical value A^*, which is somewhere in the interval $]0.48, 0.49[$. Apart from some minor deformations in the contour lines of Ω, the figure looks like Minkowski spacetime, although nonlinear effects like backscattering are already significant. The $\Omega = 0$ contour coincides with the analytic location of $\mathcal{I}$ represented by the thick dashed line. The values depending on the outer boundary of the grid have not even been calculated. That is why there are no contours in the upper triangle.

In Fig. 5 the spacetime has become singular. The thick line is certainly a singular boundary of the future domain of dependence of the initial data since here and in all the following cases scalar invariants become singular. Near the center the singularity is spacelike. Further outside its slope is numerically indistinguishable from a null line. The edgy look is an effect of the plotting program and the coarse plotting grid, which will be seen later when the singularities will be examined more thoroughly—a finer grid near the singularity showing more details will be used there.

With increasing amplitude of the initial scalar field (Fig. 6) the spacelike part of the singularity has grown. The change of the shape of the singularity on approaching the critical parameter from above suggests the following conjecture: In the critical case the singularity is a null line.

For further increasing A the outer edge of the singularity becomes spacelike. This part grows inwards and finally we get a picture like Fig. 7. Note that the contour lines of Ω are focused at the intersection of $\mathcal{I}$ with the singularity. Outside $\mathcal{I}$ the scalar Ω goes to $-\infty$; inside to ∞ on approach to the singularity. In subsection V A 2 the structure of it will be examined.

The critical case was also approached from the subcritical side. In Fig. 8 the time dependence of Ω in the center is plotted for the three subcritical values $A = 0.25$,

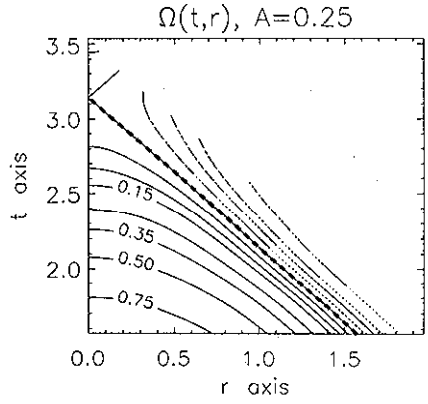

FIG. 4. $\Omega(t, r)$ for $A = 0.25$.

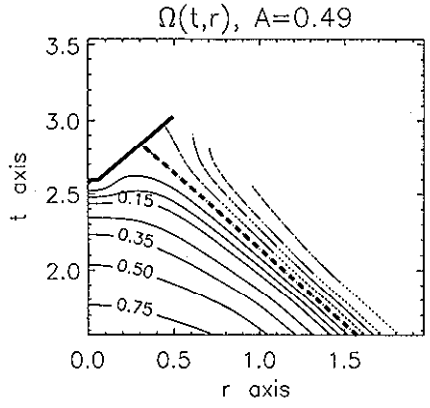

FIG. 5. $\Omega(t,r)$ for $A = 0.49$.

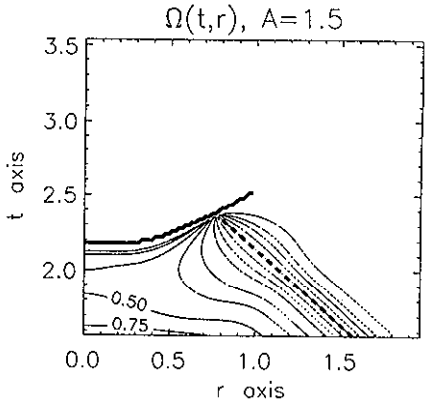

FIG. 7. $\Omega(t,r)$ for $A = 1.5$.

0.45, 0.48 and the supercritical model $A = 0.49$.

Approaching the critical case $\Omega(t,0)$ seems to develop a zero point before i^+. For spacetimes above the critical case the value of $\Omega(t,0)$ at the singularity is greater than 0 but again approaching 0 on approach to the critical case. Outside the center and away from $\mathcal{I}$, the scalar Ω does not seem to go to 0 even in the critical case. Although the values of Ω are influenced by gauge, the statement that Ω vanishes is not. The author cannot interpret this exceptional conformal structure for the critical case yet. Nevertheless the calculations show the critical model might be recognized by this behavior of Ω.

2. *Are the singularities found of physical nature?*

The figures of the preceding subsection show that there are singularities for large values of A. In subsection IIIB3 it has been described when and how the program flags a point as singular. That does not necessarily mean that those points represent a singularity in physical spacetime. In this subsection arguments will be given to decide that issue. Furthermore the quantities used classify the singularity.

In their singularity theorems Penrose and Hawking have shown that a singularity is unavoidable if there are trapped surfaces and the energy-momentum tensor fulfills certain energy conditions. The conformally invariant scalar field does not fulfill those energy conditions. Nevertheless I regard the appearance of trapped surfaces as a strong hint for singularities. With the transformation to the solution of a massless Klein-Gordon field [4] it is easy to check for the existence of an apparent horizon in a massless Klein-Gordon field model which satisfies the relevant energy conditions.

The null expansion of in- and outgoing null directions in spherical symmetry can be written as

$$\tilde{\theta}_{\text{out,in}} = \frac{1}{\tilde{r}}(\tilde{e}_{u,v}{}^a \tilde{\nabla}_a \tilde{r}) \,, \tag{20}$$

where

$$\tilde{e}_u{}^a = (\tilde{e}_{\underline{0}}{}^a + \tilde{e}_{\underline{1}}{}^a)$$

is the outgoing null vector and

$$\tilde{e}_v{}^a = (\tilde{e}_{\underline{0}}{}^a - \tilde{e}_{\underline{1}}{}^a)$$

is the ingoing null vector. Written in unphysical quantities,

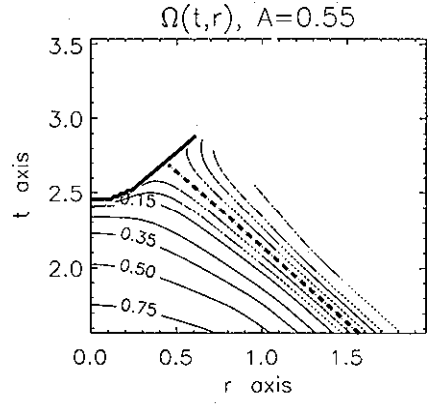

FIG. 6. $\Omega(t,r)$ for $A = 0.55$.

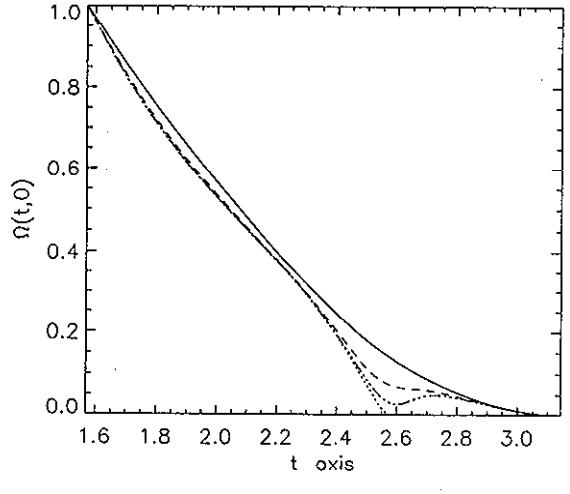

FIG. 8. $\Omega(t,0)$ for $A = 0.25$ (——), $A = 0.45$ (– – –), $A = 0.48$ (——···——), and $A = 0.49$ (· · · ·).

$$\tilde{\theta}_{\rm out} = \Omega\left(\gamma^0{}_{\underline{22}} - \frac{\gamma}{r}\right) - \Omega_{\underline{0}} - \Omega_{\underline{1}} ,$$

$$\tilde{\theta}_{\rm in} = \Omega\left(\gamma^0{}_{\underline{22}} + \frac{\gamma}{r}\right) - \Omega_{\underline{0}} + \Omega_{\underline{1}} . \qquad (21)$$

There is the freedom of null boosts; thus $\tilde{\theta}_{\rm out}$ and $\tilde{\theta}_{\rm in}$ are not gauge invariant, but their product is. On the first view one might expect that $\tilde{\theta}_{\rm out,in}$ vanish for $\tilde{r} \to \infty$. The gauge for $\tilde{e}_{u,v}$ chosen makes $\theta_{\rm out}$ not vanishing on $\mathcal{I}^+$ and $\theta_{\rm in}$ not vanishing on $\mathcal{I}^-$. That is a pure gauge effect; by an appropriate null boost $\theta_{\rm out}$ and $\theta_{\rm in}$ can be made vanishing on $\mathcal{I}$.

Another criteria for or against a "real" singularity is the behavior of curvature invariants of physical spacetime, e.g.,

$$\tilde{C}_{abcd}\tilde{C}^{abcd} = \Omega^6 d_{abcd}d^{abcd} = 12\Omega^6(d_{\underline{101}}{}^{\underline{0}})^2 .$$

Figure 9 shows the spacetime region near the singularity of a $A = 0.55$ model. The thick, dashed line is a part of $\mathcal{I}^+$, the thick line the singularity $\mathcal{S}$. The singularity is covered by a region of trapped surfaces, the thin line shows the apparent horizon. In the corresponding initial value problem for a massless Klein-Gordon field the same qualitative picture arises.

The proper time of a Bondi observer [see Eq. (25)] goes to infinity on approach to the intersection point $\mathcal{P}$ of the $\mathcal{S}$ with $\mathcal{I}^+$. This is a strong hint that $\mathcal{P}$ is a singular timelike infinity, a singular i^+. Thus the last null line from the center which reaches $\mathcal{I}^+$ at i^+ is the event horizon (dotted line).

These are already strong hints that $\mathcal{S}$ is a singularity of the physical spacetime. It is further strengthened by the fact that the curvature scalar $(\tilde{C}_{abcd}\tilde{C}^{abcd})^{1/2}$ blows up at least on approach to the inner (spacetime part) of $\mathcal{S}$. There are also hints that the area radius goes to 0 on $\mathcal{S}$, but to decide that issue more numerical accuracy near the singularity would be needed. All these considerations "prove" that $\mathcal{S}$ is a real singularity of physical spacetime.

The situation is quite different in Fig. 10. Along $\mathcal{S}$ the

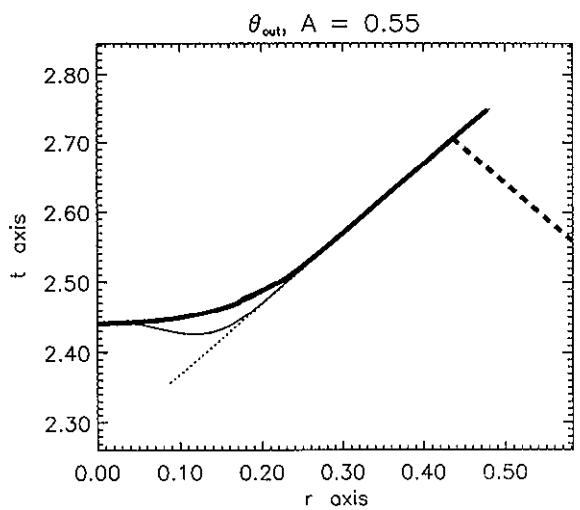

FIG. 9. $\theta_{\rm out}$ for $A = 0.55$.

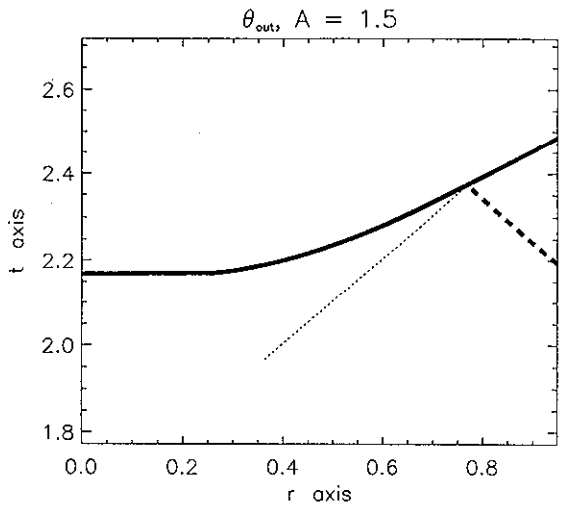

FIG. 10. $\theta_{\rm out}$ for $A = 1.5$.

scalar Ω goes to $+\infty$ inside $\mathcal{I}^+$, and to $-\infty$ outside $\mathcal{I}^+$. $\mathcal{S}$ is spacelike everywhere. $(\tilde{C}_{abcd}\tilde{C}^{abcd})^{1/2}$ does not show any sign of blow up near $\mathcal{S}$; there is no region of trapped surfaces wrapped around $\mathcal{S}$. Due to the discontinuity of Ω near $\mathcal{P}$ the formula for the proper time of an observer at $\mathcal{I}^+$ is not applicable.

Since only quantities of the unphysical spacetime become singular on $\mathcal{S}$ I conclude that $\mathcal{S}$ is a conformal singularity caused by the gauge chosen by specifying $R(t,r) = 6$. It is very similar to a coordinate singularity. Since the singularity is "unphysical" no correlation with trapped surfaces is expected. From the whole parameter study there are strong hints that the gauge singularity more and more covers the trapped surfaces and the physical singularity. Only minor, unsuccessful effort has been spent to try to avoid the conformal singularity by using different choices of $R(t,r)$.

There is another very interesting point in the models with $A \geq 1.2$. On the initial slice there are regions where both $\tilde{\theta}_{\rm in}$ and $\tilde{\theta}_{\rm out}$ are positive ("antitrapped surfaces"). A calculation back in time shows a singularity in the past, covered by an antitrapped region, i.e., a spacetime with a white hole. Although the model $A = 1.2$ shows a conformal singularity in the future the existence of an apparent horizon suggests that the physical singularity is hidden behind the conformal singularity. It is obvious to assume that beyond A^* there is always a physical singularity which is sometimes hidden by a conformal singularity.

3. *The mass scaling relation*

In his study of scalar fields Choptuik found the critical mass scaling behavior $m_{\rm BH} = a(A - A^*)^\gamma$ with a independent of A and an exponent γ of approximately 0.37. The Hawking mass

$$m(t,r) = \frac{\tilde{r}}{2}(1 + \tilde{r}^2 \tilde{\theta}_{\rm out}\tilde{\theta}_{\rm in})$$

can be written as

$$m = \frac{1}{2}\left(\frac{r}{3}\right)^3 d_{\underline{101}}{}^{\underline{0}}\left(1 - \frac{1}{4}\kappa\Omega^2\phi^2\right) + \frac{1}{8}\left(\frac{r}{e}\right)^3 \kappa\Omega \times\left\{\phi^2\left[(\gamma^{\underline{0}}{}_{\underline{22}})^2 - \left(\frac{\gamma}{r}\right)^2\right] + 2\phi\left(\gamma^{\underline{0}}{}_{\underline{22}}\phi_{\underline{0}} + \frac{\gamma}{r}\phi_{\underline{1}}\right) + [(\phi_{\underline{0}})^2 - (\phi_{\underline{1}})^2]\right\} + \frac{1}{8}\frac{r}{e}\kappa\phi^2\Omega\,. \quad (22)$$

The use of Eq. (B36) on $\mathcal{I}$ is essential to write the Hawking mass in a form not containing terms with Ω^{-1} factors. On $\mathcal{I}$ the Hawking mass is identical with the Bondi mass. For scalar field data with compact support on the initial slice in $\tilde{M}$ the Bondi mass on the initial slice coincides with the ADM mass.

Figure 11 shows a logarithmic plot of the black hole mass obtained for the parameter study performed here (the stars $*$ mark calculated models). The black hole mass is determined as the Bondi mass "at i^+." The value of 0.4866 for the critical parameter A^* has been found by optimizing the straight line look in Fig. 11.

The critical exponent is 0.37, but due to the uncertainty in A^* the error is certainly ± 0.05. Hence the results are compatible with the results of others, but I would not claim more.

Although the mass caught by the black hole increases the percentage of the caught mass has a significant maximum at $A \approx 0.75$ (see Fig. 12). For large A almost all the mass escapes to $\mathcal{I}^+$. Actually for $A >\approx 1.0$ the given value is only an upper bound since i^+ is hidden behind the conformal singularity and thus the Bondi mass at the intersection of $\mathcal{I}^+$ with the conformal singularity may further decrease. The figures for the black hole mass of the corresponding Klein-Gordon models show the same behavior.

For models with large initial scalar field amplitudes A there are number of significant changes in the structure of spacetime. Although most of the scalar field is still contained in region I the shell with most of the Hawking mass in it expands and crosses $\mathcal{I}$ in region III. Mass and scalar field "decouple" and propagation of mass is almost completely determined by nonlinear terms.

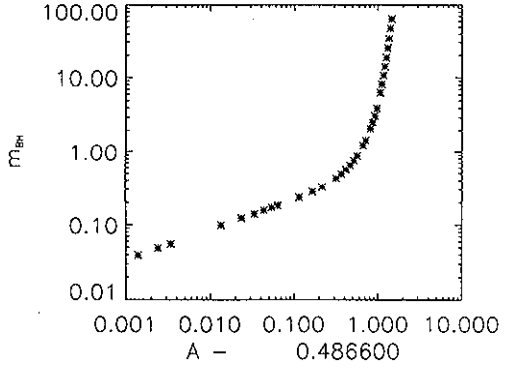

FIG. 11. Scaling relation for the black hole mass $m_{\rm BH}$.

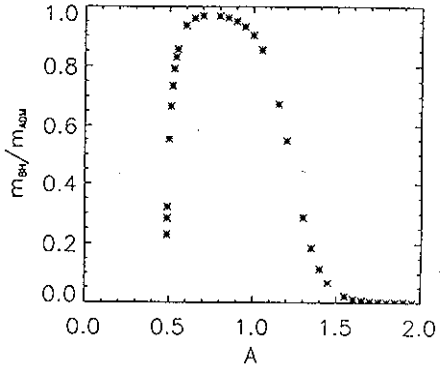

FIG. 12. Fraction of the ADM mass $m_{\rm ADM}$ caught by the black hole.

B. Christodoulou's theorem

Christodoulou investigated the general relativistic massless Klein-Gordon field in spherically symmetric spacetimes in a number of papers; for a list of references see [28]. He found sufficient conditions for the appearance of a spacetime singularity. The theorems proven there contain the following statement.

Theorem 1 [28]. Consider on the initial future null geodesic cone $\bar{C}_0^+$ an annular region bounded by the two spheres $\bar{\mathbb{S}}_{1,0}$ and $\bar{\mathbb{S}}_{2,0}$ with $\bar{\mathbb{S}}_{2,0}$ in the exterior of $\bar{\mathbb{S}}_{1,0}$ and areal radii $\bar{r}_{1,0}$ and $\bar{r}_{2,0}$. Let

$$\delta_0 := \frac{\bar{r}_{2,0}}{\bar{r}_{1,0}} - 1 \in \left(0, \frac{1}{2}\right)\,,$$

$$\eta_0 = \frac{2(\bar{m}_{2,0} - \bar{m}_{1,0})}{\bar{r}_{2,0}}\,,$$

and

$$E(y) := \frac{y}{(1+y)^2}\left[\ln\left(\frac{1}{2y}\right) + 5 - y\right]\,.$$

A sufficient condition for a nontimelike singular boundary in the future of $\bar{C}_0^+$ is

$$\eta_0 \geq E(\delta_0)\,.$$

The model with a conformal scalar field calculated here is (almost) equivalent to the massless Klein-Gordon field [4]. If $(\tilde{M}, \tilde{g}_{ab}, \tilde{\phi})$ is a solution for the general relativistic conformal scalar field model, $(\bar{M}, \bar{g}_{ab}, \bar{\phi})$ is a solution for the general relativistic massless Klein-Gordon field with

$$\bar{\phi} = \sqrt{6}\,\mathrm{arctanh}\frac{\tilde{\phi}}{2}\,, \quad (23)$$

$$\bar{g}_{ab} = \left(1 - \frac{1}{4}\tilde{\phi}^2\right)\tilde{g}_{ab}\,. \quad (24)$$

The area radius $\bar{r}$ and the Hawking mass $\bar{m}$ are given by

$$\bar{r} = \omega\tilde{r} \ ,$$

$$\bar{m} = \omega m + \frac{\tilde{r}^3}{2}\left(\tilde{\theta}_{\rm out}\tilde{e}_v(\omega) + \tilde{\theta}_{\rm in}\tilde{e}_u(\omega) + \frac{1}{\omega}\tilde{e}_v(\omega)\tilde{e}_u(\omega)\right) \ ,$$

with $\omega = \sqrt{1 - 1/4\Omega^2\phi^2}$. $\tilde{r}$ is the area radius, m the Hawking mass, and $\tilde{\theta}_{\rm out,in}$ the null expansion of the out- and ingoing null directions with null vectors $\tilde{e}_u$ and $\tilde{e}_u$ in the conformal scalar field model. $\bar{m}$ can be written in a form which does not, even implicitly, contain terms proportional to Ω^{-1}. For the purpose of this subsection it is not necessary to write $\bar{m}$ in a form obviously regular on $\mathcal{I}$.

In Fig. 13 $\eta_0 - E(\delta_0)$ is plotted for three outgoing light cones versus the area radius $\bar{r}$. For a parameter of $A = 0.75$, a model far beyond the critical value with a distinct singularity in physical spacetime, the solution has been printed out for 100 time slices with 100 grid points. On outgoing null cones $\eta_0 - E(\delta_0)$ has been evaluated. The sufficient condition is satisfied if $\eta_0 - E(\delta_0) \geq 0$. The grid points are marked with squares, diamonds, and triangles. The first light cone (squares) lies outside the event horizon; the criteria are nowhere fulfilled. The second light cone (diamonds) approximately coincides with the event horizon. The criteria are not fulfilled either. Only if the apparent horizon is crossed (triangles) $\eta_0 - E(\delta_0)$ becomes larger than 0. Although many outgoing light cones in various singular models have been checked the criteria were only fulfilled when the light cone crossed the apparent horizon. Thus I conclude that the criteria are not very sharp. This is in agreement with the results in [29].

C. Extraction of radiation

In addition to the already presented determination of the Bondi mass I am going to demonstrate the simplicity of radiation extraction on two more examples in this subsection. In the first case the effects of the nonlinearities in the equations are analyzed—the purely backscattered radiation in region III and the decay of the radiation in region II of a regular spacetime model. In the second case values of the Bondi mass in a singular model are compared with values of the mass read off at finite radii.

1. Effects of nonlinearity

Figure 14 compares ϕ on $\mathcal{I}$, i.e., the coefficient of the $1/\tilde{r}$ term of the scalar field $\tilde{\phi}$ in physical spacetime, for a model with an initial amplitude of $A = 0.40$ for the linear model ($\kappa = 0$, dotted line) and the nonlinear model ($\kappa = 1$, continuous line). In the model with gravitation a significant amount of radiation, reflected outward by backscattering, has already crossed $\mathcal{I}$ before the linear signal reaches $\mathcal{I}$ (region III). The main signal is stronger in the nonlinear case and there is some scalar field left in region II.

In Fig. 15 the Bondi mass is shown in the pure backscatter region III. Later times correspond to the backscattering of a matter shell which has decreased in size during the infall.

In Fig. 16 the scalar field ϕ is displayed in a double logarithmic plot of the scalar field versus the proper time τ of an observer at $\mathcal{I}$. This observer is obtained by taking a world line at fixed area radius $\tilde{r}$ (and angle) and taking the limit $\tilde{r} \to \infty$. In the unphysical variables one gets

$$\tau - \tau_0 = \int_{t_0}^{t} a(r_{\mathcal{I}}(t))dt \ , \qquad (25)$$

where $r_{\mathcal{I}}(t)$ is the coordinate r in unphysical spacetime of $\mathcal{I}$ at unphysical time t and

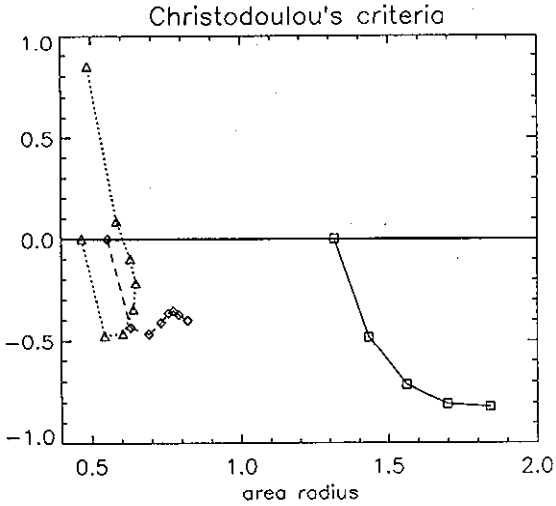

FIG. 13. Christodoulou's criteria $\eta_0 - E(\delta_0)$ versus area radius $\bar{r}$ for various light cones.

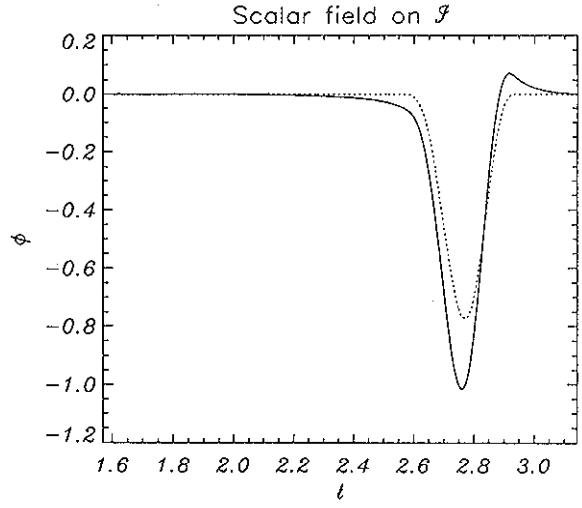

FIG. 14. ϕ for the whole time evolution.

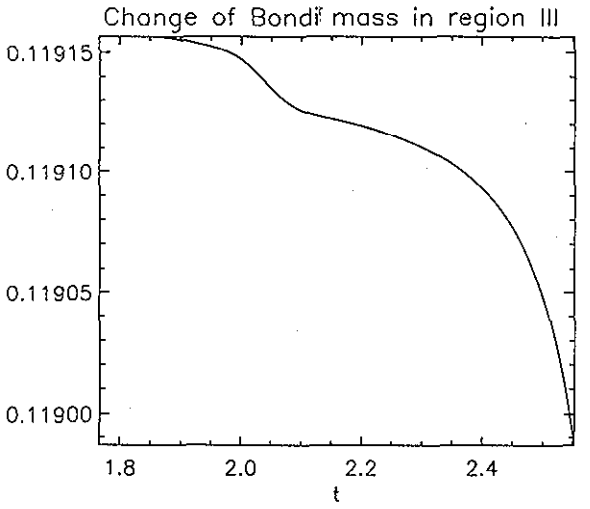

FIG. 15. m_{Bondi} in region III.

$$a = -\frac{1}{(\Omega_{\underline{1}})^2}\left[\frac{1}{(e_{\underline{0}}{}^0)^2}\left(\frac{-R-6\widehat{R2}}{12}+(\gamma 2)^2 - \frac{1}{r_{\mathcal{I}}{}^2}(e_{\underline{0}}{}^0+\gamma)^2\right)+\frac{1}{r_{\mathcal{I}}{}^2 e_{\underline{0}}{}^0}(e_{\underline{0}}{}^0+\gamma)-\frac{1}{r_{\mathcal{I}}{}^2}\right]. \quad (26)$$

The dots represent grid points of the calculation with 5000 grid points. Since on approach to i^+ the center is approached and the values become inaccurate, only those points have been included in the plot where the results of a Richardson extrapolation with 5000 and 10 000 grid points are visually indistinguishable from those of an extrapolation with 10 000 and 20 000 grid points. In this plot the last 10 (of 5000) points on $\mathcal{I}$ before i^+ are missing. The slope in the asymptotical region is approximately 0.34. Thus for very late times $\phi \sim (\tau - \tau_0)^{0.34}$.

Unfortunately the Bondi mass falls off so fast that rounding errors of the graphic program, with which the calculation of the mass is done and which has only single precision, do not allow one to enter the asymptotical region with the constant slope for ϕ. But in spite of the accuracy problem near the center, Fig. 16 illustrates an advantage of the conformal method: The time scale of the collapse of the initial matter shell is of order 1; the falloff of the decay could be investigated for almost 10^8 times the dynamical time scale.

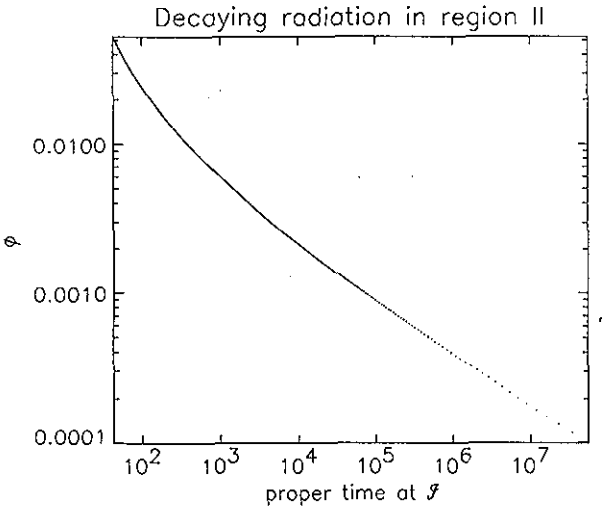

FIG. 16. ϕ in region II.

2. *Radiative quantities at finite physical distance and at $\mathcal{I}$*

A rough estimate of the errors which are to be expected by reading of radiative quantities at finite radius has been made in the following way: Given a lower bound for the area radius, the grid on a time slice has been searched for the first grid point P with larger area radius. At that point P the value for the Hawking mass $m_{\text{Haw,fin}}$ and the "finite" Bondi mass,

$$m_{\text{Bondi,fin}}(P) := \frac{1}{2}\left(\frac{r}{e}\right)^3 d_{\underline{101}}{}^{\underline{0}}\Big|_P ,$$

have been calculated. Those values have been compared with the Bondi mass on the intersection point of the future directed light cone of P and $\mathcal{I}^+$. The model used corresponds to the parameter $A = 0.55$ and develops strong gravitational fields, the spacetime has a singularity which catches approximately 85% of the ADM mass of 0.22. The outer boundary of the compact support of the scalar field lies at an area radius $\tilde{r} = 2.7$, P has been chosen at two, five, and ten times that value. P is at 10, 25, or 50 expressed in units of the ADM mass.

The maximal relative error, i.e., error over ADM mass, is approximately 2%, 1%, and 0.1%. But the relative error in the backscattering region III (error/mass loss in region III) is by a factor of 10 larger. Those errors are the errors made by approximating null infinity by a grid which ends at a finite physical distance. There is almost no difference between $m_{\text{Haw,fin}}$ and $m_{\text{Bondi,fin}}$.

VI. SUMMARY

In the work reported in this paper a mathematical formalism, designed to investigate the structure of a spacetime in the large by conformal techniques, has been introduced into numerics. This paper demonstrates that global properties of a spacetime are numerically calculable and must not necessarily be estimated from a numerical simulation by heuristic arguments.

The set of equations can be solved either by a spacetime or a characteristic initial value problem. The form of the equations differs from Einstein's equations. The technical tricks developed for the numerical solution of Einstein's equations cannot be used unchanged. The accuracy problem as described in Sec. IV B shows that there is still the potential for further progress. Recently, too late to be included in this paper, a new way of dis-

cretizing was found, which propagates the regularity condition at the center without switching schemes near the center, as done here. The accuracy has improved by a factor of 10 for models near the critical parameter.

In this formalism important properties of spacetimes are automatically fulfilled, the ADM mass is always conserved, the energy radiated away equals the change in the Bondi mass, and there is no spurious ingoing wave caused by an unphysical reflection at the outer boundary. Furthermore the location of event horizons is straightforward and the calculation yields "Penrose" diagrams allowing one to read off the causal structure of singularities.

The obvious advantages might not be worth the effort for the investigation of astrophysical questions where most of the uncertainty originates in an approximate equation of state. But if one is interested in the use of numerical relativity as a substitute for the lacking experimental approach to the open problems of mathematical relativity, the conformal techniques provide a very promising approach. In this circumstance it should be mentioned that Friedrich has developed the conformal techniques further [30]. There the rescaling factor Ω is no longer a variable of the system fixed in a complicated way by the gauge source function $R(t,r)$. The gauge freedom in the rescaling is fixed directly by specifying $\Omega(t,r)$. The approach is used by Friedrich [31] to investigate the structure of i^0 for special choices of data.

ACKNOWLEDGMENTS

It is a pleasure for me to thank the relativity group in Garching for the cooperation during my Ph.D. thesis, J. Winicour and J. Stewart for their advice on my first steps in numerical relativity during their stays in Garching, and W. Kley for helpful comments on the manuscript.

APPENDIX A: NOTATION

The signature of the Lorentzian metric g_{ab} is $(-,+,+,+)$. Whenever possible I use abstract indices as described in [32, Chap. 2]. Small Latin letters denote abstract indices, underlined small Latin letters are frame indices. For the components of a tensor with respect to coordinates small Greek letters are used. The frame $(\partial/\partial x^\mu)^a$ is constructed from the coordinate x^μ, ${e_{\underline{i}}}^a$ denotes an arbitrary frame. In this notation v_a is a covector, $v_{\underline{i}}$ a scalar, namely $v_a {e_{\underline{i}}}^a$. $v(f)$ is defined to be the action of the vector v^a on the function f, i.e., for every covariant derivative $\nabla_a : t(f) = t^a \nabla_a f$.

The transformation between abstract, coordinate, and frame indices is done by contracting with ${e_{\underline{i}}}^a$ and ${e_{\underline{i}}}^\mu$. All indices may be raised and lowered with the metric g_{AB} and the inverse g^{AB}, $g^{AC}g_{CB} = \delta^A{}_B$; A and B are arbitrary indices, e.g., $e_{\underline{i}a} = g_{ab}{e_{\underline{i}}}^b$ and ${e^{\underline{i}}}_a = g^{\underline{ij}}e_{\underline{j}a}$.

For a frame ${e_{\underline{i}}}^a$ and a covariant derivative ∇_a the Ricci rotation coefficients are defined as

$$\gamma^a{}_{\underline{ij}} := {e_{\underline{i}}}^b \nabla_b {e_{\underline{j}}}^a .$$

From this definition follows

$${e_{\underline{i}}}^a {e^{\underline{j}}}_b (\nabla_a t^b) = e_{\underline{i}}(t^{\underline{j}}) + \gamma^{\underline{j}}{}_{\underline{ik}} t^{\underline{k}} .$$

With respect to a coordinate frame ${e_\mu}^a \equiv (\partial/\partial x^\mu)^a$ the components $\gamma^\lambda{}_{\mu\nu}$ are the Christoffel symbols $\Gamma^\lambda{}_{\mu\nu}$.

The torsion $T^a{}_{bc}$ is defined by

$$\nabla_a \nabla_b f - \nabla_b \nabla_a f = -T^c{}_{ab} \nabla_c f$$

and the Riemann tensor $R_{abc}{}^d$ by

$$\nabla_a \nabla_b \omega_c - \nabla_b \nabla_a \omega_c = R_{abc}{}^d \omega_d - T^d{}_{ab} \nabla_d \omega_c .$$

Contraction gives the Ricci tensor,

$$R_{ab} = R_{acb}{}^c ,$$

and the Ricci scalar,

$$R = R_{ab} g^{ab} .$$

The Einstein tensor is given by

$$G_{ab} = R_{ab} - \tfrac{1}{2} R g_{ab} .$$

The speed of light c is set to 1. The gravitational constant κ in $G_{ab} = \kappa T_{ab}$ has been set to 1 or 0 in the calculations, corresponding to the full nonlinear theory or a scalar field on a flat background, respectively.

APPENDIX B: THE SYSTEM OF EQUATIONS IN DOUBLE NULL COORDINATES

1. The time evolution equations

From the system (2) the following set of equations can be derived, where the abbreviations

$$\gamma 1 = \gamma^0{}_{\underline{01}} + \gamma^0{}_{\underline{11}} ,$$

$$\gamma 2 = \gamma^0{}_{\underline{22}} ,$$

$$\gamma 3 = \gamma^0{}_{\underline{11}} - \gamma^0{}_{\underline{01}} ,$$

$$\widehat{R1} = (\hat{R}_{\underline{01}} + \hat{R}_{\underline{11}})/2 ,$$

$$\widehat{R2} = \hat{R}_{\underline{00}} - \hat{R}_{\underline{11}} ,$$

$$\widehat{R3} = (\hat{R}_{\underline{11}} - \hat{R}_{\underline{01}})/2 ,$$

$$\widehat{\phi 1} = (\hat{\phi}_{\underline{01}} + \hat{\phi}_{\underline{11}}/2 ,$$

$$\widehat{\phi 3} = (\hat{\phi}_{\underline{11}} - \hat{\phi}_{\underline{01}})/2 , \qquad \text{(B1)}$$

and the substitutions

$$\phi_a{}^a \to \frac{R}{6} ,$$

$$\omega \to \frac{1}{4}\Omega\widehat{R2} - \frac{1}{4}\Omega^3(\hat{T}_{\underline{00}} - \hat{T}_{\underline{11}}) - \gamma 2\,\Omega_{\underline{0}} - \frac{\gamma}{r}\Omega_{\underline{1}} ,$$

and

$$\phi 2 = \hat{\phi}_{\underline{00}} - \hat{\phi}_{\underline{11}} \to -2\gamma 2\,\phi_{\underline{0}} - 2\frac{\gamma}{r}\phi_{\underline{1}} - \frac{1}{2}\phi_a{}^a , \quad \text{(B2)}$$

which follow from spherical symmetry, have been used:

$$(\partial_{\underline{0}} + \partial_{\underline{1}})\gamma 3 = -(\gamma 3\gamma 1) + d_{\underline{101}}{}^{\underline{0}}\Omega + \frac{1}{2}\left(\frac{R}{6} - \widehat{R2}\right) , \quad \text{(B3)}$$

$$(\partial_{\underline{0}} + \partial_{\underline{1}})\widehat{R3} = (d_{\underline{101}}{}^{\underline{0}}\Omega_{\underline{0}} + \Omega m + S_{\widehat{R3}})/[1 - \kappa(\Omega\phi/2)^2] + [-\gamma 1(\tfrac{1}{2}\widehat{R2} + 2\widehat{R3}) + \gamma 2(\widehat{R1} - \widehat{R3}) + \tfrac{1}{8}(\partial_{\underline{1}}R) - \tfrac{1}{24}(\partial_{\underline{0}}R)] , \quad \text{(B4)}$$

with

$$S_{\widehat{R3}} = \begin{cases} \gamma\{[1 - \kappa(\Omega\phi/2)^2](\widehat{R1} + \widehat{R3} - \frac{1}{2}\widehat{R2})/r - \frac{\kappa}{2}\Omega(\phi_{\underline{1}}/r)(\Omega_{\underline{0}}\phi + \phi_{\underline{0}}\Omega)\} & \text{for } r \neq 0 , \\ -\frac{\kappa}{2}\gamma\Omega(\Omega_{\underline{0}}\phi + \phi_{\underline{0}}\Omega)\partial_r\phi_{\underline{1}} & \text{for } r = 0 , \end{cases} \quad \text{(B5)}$$

$$(\partial_{\underline{0}} + \partial_{\underline{1}})\widehat{\phi 3} = \gamma 2(\widehat{\phi 1} - \widehat{\phi 3}) - 2\gamma 1\,\widehat{\phi 3} + \frac{\phi_{\underline{0}}}{2}\left(-(\widehat{R1} - \widehat{R3}) - d_{\underline{101}}{}^{\underline{0}}\Omega + \frac{1}{2}\widehat{R2} - \frac{1}{8}R + 2\gamma 2\,\gamma 1\right) + \frac{\phi_{\underline{1}}}{2}\left(\widehat{R1} + \widehat{R3} + \frac{3}{8}R\right) + \phi\left(\frac{1}{16}(\partial_{\underline{1}}R) + \frac{1}{24}\gamma 1\,R - \frac{1}{48}(\partial_{\underline{0}}R)\right) + S_{\widehat{\phi 3}} , \quad \text{(B6)}$$

$$S_{\widehat{\phi 3}} = \begin{cases} \gamma\{[(\phi_{\underline{1}}/r)\gamma + \gamma 2\,\phi_{\underline{0}} + \frac{1}{24}\phi R + \widehat{\phi 1} + \widehat{\phi 3}]/r + \gamma 1(\phi_{\underline{1}}/r)\} & \text{for } r \neq 0 , \\ \gamma\,\gamma 1\,\partial_r\phi_{\underline{1}} & \text{for } r = 0 , \end{cases}$$

$$(\partial_{\underline{0}} - \partial_{\underline{1}})\gamma 1 = -(\gamma 3\,\gamma 1) + d_{\underline{101}}{}^{\underline{0}}\Omega + \frac{1}{2}\left(\frac{R}{6} - \widehat{R2}\right) , \quad \text{(B7)}$$

$$(\partial_{\underline{0}} - \partial_{\underline{1}})\widehat{R1} = (d_{\underline{101}}{}^{\underline{0}}\Omega_{\underline{0}} + \Omega m + S_{\widehat{R1}})/[1 - \kappa(\Omega\phi/2)^2] + [-\gamma 3(\tfrac{1}{2}\widehat{R2} + 2\widehat{R1}) - \gamma 2(\widehat{R1} - \widehat{R3}) - \tfrac{1}{8}(\partial_{\underline{1}}R) - \tfrac{1}{24}(\partial_{\underline{0}}R)] , \quad \text{(B8)}$$

$$S_{\widehat{R1}} = \begin{cases} \gamma\{-[1 - \kappa(\Omega\phi/2)^2](\widehat{R1} + \widehat{R3} - \frac{1}{2}\widehat{R2})/r - \frac{\kappa}{2}\Omega(\phi_{\underline{1}}/r)(\Omega_{\underline{0}}\phi + \phi_{\underline{0}}\Omega)\} & \text{for } r \neq 0 , \\ -\frac{\kappa}{2}\gamma\Omega(\Omega_{\underline{0}}\phi + \phi_{\underline{0}}\Omega)\partial_r\phi_{\underline{1}} & \text{for } r = 0 , \end{cases}$$

$$(\partial_{\underline{0}} - \partial_{\underline{1}})\widehat{\phi 1} = -\gamma 2(\widehat{\phi 1} - \widehat{\phi 3}) - 2\widehat{\phi 1}\gamma 3 + \frac{\phi_{\underline{0}}}{2}\left(\widehat{R1} - \widehat{R3} - d_{\underline{101}}{}^{\underline{0}}\Omega + \frac{1}{2}\widehat{R2} - \frac{1}{8}R + 2\gamma 3\,\gamma 2\right) + \frac{\phi_{\underline{1}}}{2}\left(-(\widehat{R1} + \widehat{R3}) - \frac{3}{8}R\right) + \phi\left(-\frac{1}{16}(\partial_{\underline{1}}R) + \frac{1}{24}\gamma 3\,R - \frac{1}{48}(\partial_{\underline{0}}R)\right) + S_{\widehat{\phi 1}} , \quad \text{(B9)}$$

$$S_{\widehat{\phi 1}} = \begin{cases} \gamma\{-[(\phi_{\underline{1}}/r)\gamma + \gamma 2\,\phi_{\underline{0}} + \frac{1}{24}\phi R + \widehat{\phi 1} + \widehat{\phi 3}]/r + (\phi_{\underline{1}}/r)\gamma 3\} & \text{for } r \neq 0 , \\ \gamma\,\gamma 1\,\partial_r\phi_{\underline{1}} & \text{for } r = 0 , \end{cases}$$

$$\partial_{\underline{0}}e_{\underline{0}}{}^0 = -\tfrac{1}{2}e_{\underline{0}}{}^0(\gamma 3 + \gamma 1) , \quad \text{(B10)}$$

$$\partial_{\underline{0}}e = -e\gamma 2 , \quad \text{(B11)}$$

$$\partial_{\underline{0}}\gamma 2 = -(\gamma 2)^2 - \frac{1}{2}d_{\underline{101}}{}^{\underline{0}}\Omega + \frac{1}{2}\left(-(\widehat{R1} + \widehat{R3}) - \frac{1}{2}\widehat{R2} + \frac{R}{6}\right) + S_{\gamma 2} , \quad \text{(B12)}$$

$$S_{\gamma 2} = \begin{cases} \frac{\gamma}{2}(\gamma 3 - \gamma 1)/r & \text{for } r \neq 0 \,, \\ \frac{\gamma}{2}\partial_r(\gamma 3 - \gamma 1) & \text{for } r = 0 \,, \end{cases}$$

$$\partial_{\underline{0}}\gamma = -\gamma 2\,\gamma + \frac{r}{2}[(\gamma 3 - \gamma 1)\gamma 2 + (\widehat{R1} - \widehat{R3})] \,, \tag{B13}$$

$$\partial_{\underline{0}}\widehat{R2} = [-2(\Omega m + d_{\underline{101}}{}^{\underline{0}}\Omega_{\underline{0}}) + S_{\widehat{R2}}]/[1 - \kappa(\Omega\phi/2)^2] + \left(\gamma 2[-2(\widehat{R1} + \widehat{R3}) - 3\widehat{R2}] - \tfrac{1}{6}(\partial_{\underline{0}}R)\right) \,, \tag{B14}$$

$$S_{\widehat{R2}} = \begin{cases} \gamma\{-2[1 - \kappa(\Omega\phi/2)^2](\widehat{R1} - \widehat{R3})/r + \kappa\Omega(\phi_{\underline{1}}/r)(\Omega_{\underline{0}}\phi + \phi_{\underline{0}}\Omega)\} & \text{for } r \neq 0 \,, \\ \gamma\{-2[1 - \kappa(\Omega\phi/2)^2]\partial_r(\widehat{R1} - \widehat{R3}) + \kappa\Omega(\Omega_{\underline{0}}\phi + \phi_{\underline{0}}\Omega)\partial_r\phi_{\underline{1}}\} & \text{for } r = 0 \,, \end{cases}$$

$$\partial_{\underline{0}}\Omega = \Omega_{\underline{0}} \,, \tag{B15}$$

$$\partial_{\underline{0}}\Omega_{\underline{0}} = \gamma 2\Omega_{\underline{0}} - \frac{1}{2}(\gamma 3 - \gamma 1)\Omega_{\underline{1}} + \Omega\left\{\frac{\kappa}{4}\Omega^2\left[\phi\left(\frac{R}{8}\phi - (\widehat{\phi 1} + \widehat{\phi 3})\right) + \phi_{\underline{0}}(3\gamma 2\,\phi + 2\phi_{\underline{0}})\right.\right.$$
$$\left.\left. -\frac{1}{2}\left((\widehat{R1} + \widehat{R3}) + \frac{3}{2}\widehat{R2}\right)[1 - \kappa(\Omega\phi/2)^2]\right]\right\} + S_{\Omega_{\underline{0}}} \,, \tag{B16}$$

$$S_{\Omega_{\underline{0}}} = \begin{cases} \gamma[\Omega_{\underline{1}}/r + \frac{3}{4}\kappa\Omega^3\phi(\phi_{\underline{1}}/r)] & \text{for } r \neq 0 \,, \\ \gamma\left(\partial_r\Omega_{\underline{1}} + \frac{3}{4}\kappa\Omega^3\phi\partial_r\phi_{\underline{1}}\right) & \text{for } r = 0 \,, \end{cases}$$

$$\partial_{\underline{0}}\Omega_{\underline{1}} = -\frac{1}{2}[1 - \kappa(\Omega\phi/2)^2](\widehat{R1} - \widehat{R3})\Omega + \frac{\kappa}{2}\Omega^3\left(\phi_{\underline{0}}\phi_{\underline{1}} - \frac{1}{2}(\widehat{\phi 1} - \widehat{\phi 3})\phi\right) - \frac{1}{2}(\gamma 3 - \gamma 1)\Omega_{\underline{0}} \,, \tag{B17}$$

$$\partial_{\underline{0}} = \phi_{\underline{0}} \,, \tag{B18}$$

$$\partial_{\underline{0}}\phi_{\underline{0}} = -2\gamma 2\,\phi_{\underline{0}} - \frac{\phi_{\underline{1}}}{2}(\gamma 3 - \gamma 1) - \phi\frac{R}{8} + \widehat{\phi 1} + \widehat{\phi 3} + S_{\phi_{\underline{0}}} \,, \tag{B19}$$

$$S_{\phi_{\underline{0}}} = \begin{cases} -2\gamma(\phi_{\underline{1}}/r) & \text{for } r \neq 0 \,, \\ -2\gamma\partial_r\phi_{\underline{1}} & \text{for } r = 0 \,, \end{cases} \tag{B20}$$

$$\partial_{\underline{0}}\phi_{\underline{1}} = \widehat{\phi 1} - \widehat{\phi 3} - \frac{\phi_{\underline{0}}}{2}(\gamma 3 - \gamma 1) \,,$$

$$\partial_{\underline{0}}d_{\underline{101}}{}^{\underline{0}} = -3\gamma 2\,d_{\underline{101}}{}^{\underline{0}} + \left(m + \frac{\kappa}{4}\phi^2\Omega_{\underline{0}}\Omega d_{\underline{101}}{}^{\underline{0}} + S_{d_{\underline{101}}{}^{\underline{0}}}\right)\Big/[1 - \kappa(\Omega\phi/2)^2] \,, \tag{B21}$$

$$S_{d_{\underline{101}}{}^{\underline{0}}} = \begin{cases} -\gamma\frac{\kappa}{2}(\phi_{\underline{1}}/r)(\Omega_{\underline{0}}\phi + \Omega\phi_{\underline{0}}) & \text{for } r \neq 0 \,, \\ -\gamma\frac{\kappa}{2}(\Omega_{\underline{0}}\phi + \Omega\phi_{\underline{0}})\partial_r\phi_{\underline{1}} & \text{for } r = 0 \,, \end{cases}$$

where m stands for

$$m = \frac{\kappa}{2}(\phi\Omega_{\underline{1}} + \phi_{\underline{1}}\Omega)(\widehat{\phi 1} - \widehat{\phi 3}) - \frac{\kappa}{2}(\phi\Omega_{\underline{0}} + \phi_{\underline{0}}\Omega)(\widehat{\phi 1} + \widehat{\phi 3}) + \frac{\kappa}{4}\phi_{\underline{1}}[4\Omega_{\underline{0}}\phi_{\underline{1}} - \phi\Omega(\widehat{R1} - \widehat{R3})]$$
$$+\kappa\phi_{\underline{0}}\left\{\frac{1}{4}\phi\left[-2\gamma 2\,\Omega_{\underline{0}} + \Omega\left(d_{\underline{101}}{}^{\underline{0}}\Omega + (\widehat{R1} + \widehat{R3} - \tfrac{1}{2}\widehat{R2}) - \frac{1}{12}R\right)\right] - \frac{1}{2}\gamma 2\,\Omega\phi_{\underline{0}} - \Omega_{\underline{1}}\phi_{\underline{1}}\right\}$$
$$+\frac{\kappa}{4}\phi^2\left[-\Omega_{\underline{1}}(\widehat{R1} - \widehat{R3}) + \Omega_{\underline{0}}\left((\widehat{R1} + \widehat{R3} - \tfrac{1}{2}\widehat{R2}) - \frac{1}{12}R\right)\right] \,.$$

2. The constraints

From (2) the following set of constraint equations can be derived:

$$\partial_{\underline{1}} e_{\underline{0}}{}^0 = -\tfrac{1}{2}(\gamma 3 - \gamma 1) \ , \tag{B22}$$

$$\partial_{\underline{1}} e = e\frac{e_{\underline{0}}{}^0 + \gamma}{r} \quad \text{for } r \neq 0, \ 0 \text{ otherwise} \ , \tag{B23}$$

$$\partial_{\underline{1}}\gamma 2 = \frac{1}{2}(\widehat{R3} - \widehat{R1}) + \frac{\gamma}{r}\left(\gamma 2 - \frac{1}{2}(\gamma 1 + \gamma 3)\right)$$

$$\text{for } r \neq 0, \ 0 \text{ otherwise} \ , \tag{B24}$$

$$\partial_{\underline{1}}\gamma = \gamma\frac{e_{\underline{0}}{}^0 + \gamma}{r} + \frac{r}{2}\left(\frac{R}{6} + \widehat{R1} + \frac{\widehat{R2}}{2} + \widehat{R3} - d_{\underline{101}}{}^{\underline{0}}\Omega - (\gamma 1 + \gamma 3)\gamma 2\right) \quad \text{for } r \neq 0, \ 0 \text{ otherwise} \ , \tag{B25}$$

$$\partial_{\underline{1}}\widehat{R2} = 2\gamma 2(\widehat{R3} - \widehat{R1}) - \tfrac{1}{6}(\partial_{\underline{1}} R) + [-2(\Omega m_C + d_{\underline{101}}{}^{\underline{0}}\Omega_{\underline{1}}) + s_{\widehat{R2}}]/[1 - \kappa(\Omega\phi/2)^2] \ ,$$

$$s_{\widehat{R2}} = \gamma\{-2[1 - \kappa(\Omega\phi/2)^2](\widehat{R1} + \widehat{R3} - \tfrac{1}{2}\widehat{R2})/r + 3\kappa\Omega(\phi_{\underline{1}}/r)(\Omega_{\underline{1}}\phi + \phi_{\underline{1}}\Omega)\}$$

$$\text{for } r \neq 0, \ 0 \text{ otherwise} \ , \tag{B26}$$

$$\partial_{\underline{1}}\Omega = \Omega_{\underline{1}} \ , \tag{B27}$$

$$\partial_{\underline{1}}\Omega_{\underline{0}} = \Omega_{\underline{1}}\frac{\gamma 3 + \gamma 1}{2} - \frac{\widehat{R1} - \widehat{R3}}{2}\Omega + \frac{\kappa}{4}\Omega^3\left(2\phi_{\underline{0}}\phi_{\underline{1}} + \phi(\widehat{\phi 3} - \widehat{\phi 1}) + \frac{\phi^2}{2}(\widehat{R1} - \widehat{R3})\right) \ , \tag{B28}$$

$$\partial_{\underline{1}}\Omega_{\underline{1}} = \left(\frac{\gamma 1 + \gamma 3}{2} - \gamma 2\right)\Omega_{\underline{0}} - \frac{\gamma}{r}\Omega_{\underline{1}} - \frac{\Omega}{2}\left(\widehat{R1} - \frac{\widehat{R2}}{2} + \widehat{R3}\right) + \frac{\kappa}{4}\Omega^3\left\{2(\phi_{\underline{1}})^2 + \phi\left[\widehat{\phi 3} - \widehat{\phi 1} - \gamma 2\,\phi_{\underline{0}} - \frac{\gamma}{r}\phi_{\underline{1}} + \frac{\phi}{2}\left(\widehat{R1} - \frac{\widehat{R2}}{2} + \widehat{R3} - \frac{R}{12}\right)\right]\right\} \quad \text{for } r \neq 0 \ , \tag{B29}$$

$$\partial_{\underline{1}}\phi = \phi_{\underline{1}} \ , \tag{B30}$$

$$\partial_{\underline{1}}\phi_{\underline{0}} = \widehat{\phi 1} - \widehat{\phi 3} + \frac{\gamma 3 + \gamma 1}{2}\phi_{\underline{1}} \ , \tag{B31}$$

$$\partial_{\underline{1}}\phi_{\underline{1}} = \widehat{\phi 1} + \widehat{\phi 3} + \frac{\gamma 3 + \gamma 1}{2}\phi_{\underline{0}} + \frac{R}{24}\phi \ , \tag{B32}$$

$$\partial_{\underline{1}} d_{\underline{101}}{}^{\underline{0}} = \left(m_C + \frac{\kappa}{4}\phi^2\Omega_{\underline{1}}\Omega d_{\underline{101}}{}^{\underline{0}} + s_{d_{\underline{101}}{}^{\underline{0}}}\right)/[1 - \kappa(\Omega\phi/2)^2] \ , \tag{B33}$$

$$s_{d_{\underline{101}}{}^{\underline{0}}} = \gamma\left[3\kappa\left([1 - \kappa(\Omega\phi/2)^2]d_{\underline{101}}{}^{\underline{0}}/r - \frac{\kappa}{2}\phi_{\underline{1}}/r(\Omega\phi_{\underline{1}} + \Omega_{\underline{1}}\phi)\right)\right] \quad \text{for } r \neq 0 \ , \tag{B34}$$

where m_C stands for

$$m_C = \frac{\kappa}{2}(\phi\Omega_{\underline{1}} + \phi_{\underline{1}}\Omega)(\widehat{\phi 1} + \widehat{\phi 3}) - \frac{\kappa}{2}(\phi\Omega_{\underline{0}} + \phi_{\underline{0}}\Omega)(\widehat{\phi 1} - \widehat{\phi 3}) + \frac{\kappa}{4}\phi_{\underline{0}}[4\Omega_{\underline{0}}\phi_{\underline{1}} - 4\Omega_{\underline{1}}\phi_{\underline{0}} - 6\gamma 2\,\Omega_{\underline{1}}\phi + \phi\Omega(\widehat{R1} - \widehat{R3})]$$
$$+\kappa\phi_{\underline{1}}\left\{\frac{1}{4}\phi\Omega\left[d_{\underline{101}}{}^{\underline{0}}\Omega - \left(\widehat{R1} + \widehat{R3} - \frac{3}{2}\widehat{R2}\right) - \frac{1}{4}R\right] - 6\gamma 2\,\Omega\phi_{\underline{0}}\right.$$
$$\left.+\frac{\kappa}{4}\phi^2\left[\Omega_{\underline{0}}(\widehat{R1} - \widehat{R3}) - \Omega_{\underline{1}}\left(\widehat{R1} + \widehat{R3} + \frac{3}{2}\widehat{R2}\right) + \frac{1}{4}R\right]\right\} . \tag{B35}$$

Equation (4), which must be fulfilled at one point, becomes

$$R\Omega^2 + 6\widehat{R2}\Omega^2 - 24\gamma 2\,\Omega\Omega_{\underline{0}} + 12{\Omega_{\underline{0}}}^2 - 24\frac{\gamma}{r}\Omega\Omega_{\underline{1}} - 12{\Omega_{\underline{1}}}^2 - \frac{\kappa}{4}R\Omega^4\phi^2$$

$$-\frac{3}{2}\kappa\widehat{R2}\Omega^4\phi^2 - 6\kappa\gamma 2\,\Omega^4\hat{\phi}\phi_{\underline{0}} - 3\kappa\Omega^4{\phi_{\underline{0}}}^2 - 6\kappa\frac{\gamma}{r}\Omega^4\phi\phi_{\underline{1}} + 3\kappa\Omega^4{\phi_{\underline{1}}}^2 = 0\,. \quad \text{(B36)}$$

Because of spherical symmetry there is also the identity

$$\Omega d_{\underline{101}}{}^{\underline{0}} = \frac{e^2-\gamma^2}{r^2} + (\gamma 2)^2 - \frac{1}{2}\widehat{R2} - \frac{R}{12}\,. \quad \text{(B37)}$$

3. The regularity conditions

At the center the following must hold for a regular spacetime:

$$e = -\gamma = e_{\underline{1}}{}^{\underline{1}}\,, \quad \text{(B38a)}$$

$$\gamma 3 = \gamma 1\,, \quad \text{(B38b)}$$

$$\gamma 2 = \tfrac{1}{2}(\gamma 3 + \gamma 1)\,, \quad \text{(B38c)}$$

$$\widehat{R1} = \widehat{R3}\,, \quad \text{(B38d)}$$

$$\widehat{R2} = 2(\widehat{R1} + \widehat{R3})\,, \quad \text{(B38e)}$$

$$d_{\underline{101}}{}^{\underline{0}} = 0\,, \quad \text{(B38f)}$$

$$\Omega_{\underline{1}} = 0\,, \quad \text{(B38g)}$$

$$\phi_{\underline{1}} = 0\,, \quad \text{(B38h)}$$

$$\widehat{\phi 1} = \widehat{\phi 3}\,. \quad \text{(B38i)}$$

On $\mathcal{I}$

$$\Omega_{\underline{0}} - \Omega_{\underline{1}} = 0\,, \quad \text{(B38j)}$$

$$\widehat{R1} + \widehat{R3} = \frac{1}{\Omega_{\underline{1}}}\Bigg\{-\partial_{\underline{1}}\partial_{\underline{1}}\Omega_{\underline{1}} - \frac{\gamma}{r}\partial_{\underline{1}}\Omega_{\underline{1}} + \frac{\gamma 3+\gamma 1}{2}\left(\frac{\gamma 3+\gamma 1}{2} - \gamma 2\right)$$
$$+\frac{\Omega_{\underline{0}}}{2}(\widehat{R1} - \widehat{R3}) - \Omega_{\underline{1}}\frac{R}{12} + \Omega_{\underline{1}}\left[\frac{\gamma 3+\gamma 1}{2}\gamma 2 - \left(\frac{\gamma}{r}\right)^2\right] + \Omega_{\underline{0}}\left[\partial_{\underline{1}}\frac{\gamma 3+\gamma 1}{2} + \left(\frac{\gamma 3+\gamma 1}{2} - \gamma 2\right)\frac{\gamma}{r}\right]\Bigg\}\,. \quad \text{(B38k)}$$

Equation (B38j) also guarantees that equation (B36) is satisfied on at least one point in M, namely $\mathcal{I}$.

[1] S. W. Hawking and G. F. R. Ellis, *The Large Scale Structure of Space-Time*, Cambridge Monographs on Mathematical Physics (Cambridge University Press, Cambridge, England, 1973).

[2] D. Christodoulou and S. Klainerman, *The Global Nonlinear Stability of the Minkowski Space* (Princeton University Press, Princeton, NJ, 1993).

[3] H. Friedrich, J. Diff. Geom. **34**, 275 (1991).

[4] P. Hübner, Class. Quantum Grav. **12**, 791 (1995).

[5] M. W. Choptuik, Phys. Rev. Lett. **70**, 9 (1993).

[6] C. J. S. Clarke, Class. Quantum Grav. **11**, 1375 (1994).

[7] H. Bondi, M. G. J. van der Burg, and A. W. K. Metzner, Proc. R. Soc. London **A269**, 21 (1962).

[8] R. Geroch, in *Asymptotic Structure of Space-Time*, edited by F. R. Esposito and L. Witten (Plenum, New York, 1976), pp. 1–105.

[9] R. Penrose, in *Relativity, Groups and Topology*, edited by C. DeWitt and B. DeWitt (Gordon and Breach, New York, 1964), pp. 565–584.

[10] H. Friedrich, Proc. R. Soc. London **A375**, 169 (1981).

[11] H. Friedrich, Commun. Math. Phys. **91**, 445 (1983).

[12] H. Friedrich, Commun. Math. Phys. **100**, 445 (1985).

[13] H. Friedrich, Commun. Math. Phys. **103**, 35 (1986).

[14] H. Friedrich, Commun. Math. Phys. **107**, 587 (1986).

[15] H. Friedrich, Commun. Math. Phys. **119**, 51 (1988).
[16] R. M. Wald, *General Relativity* (University of Chicago Press, Chicago, 1984).
[17] M. W. Choptuik, in *Approaches to Numerical Relativity*, Proceedings of the International Workshop on Numerical Relativity, edited by R. d'Inverno (Cambridge University Press, Cambridge, England, 1992), pp. 202–222.
[18] P. Hübner, Ph.D. thesis, Ludwig-Maximilians-Universität München, 1993.
[19] U. Proff, Ph.D. thesis, Universität Köln, 1985.
[20] L. Andersson, P. T. Chrusciel, and H. Friedrich, Commun. Math. Phys. **149**, 587 (1992).
[21] W. H. Press, B. P. Flannery, S. A. Teukolsky, and W. T. Vetterling, *Numerical Recipes in C* (Cambridge University Press, Cambridge, England, 1988).
[22] C. Bona and J. Massó, in *Approaches to Numerical Relativity*, Proceedings of the International Workshop on Numerical Relativity, edited by R. d'Inverno (Cambridge University Press, Cambridge, England, 1992), pp. 258–264.
[23] S. L. Shapiro and S. A. Teukolsky, in *Dynamical Spacetimes and Numerical Relativity*, edited by J. M. Centrella (Cambridge University Press, Cambridge, England, 1986), pp. 74–100.
[24] J. M. Bardeen and T. Piran, Phys. Rep. **96**, 205 (1983).
[25] R. Peyret and T. D. Taylor, *Computational Methods for Fluid Flow*, Springer Series in Computational Physics (Springer-Verlag, New York, 1983).
[26] M. W. Choptuik, Phys. Rev. D **44**, 3124 (1991).
[27] C. R. Evans, in *Dynamical Spacetimes and Numerical Relativity*, edited by J. M. Centrella (Cambridge University Press, Cambridge, England, 1986), pp. 7–39.
[28] D. Christodoulou, Commun. Pure Appl. Math. **XLIV**, 339 (1991).
[29] R. Gómez and J. Winicour, in *Approaches to Numerical Relativity*, Proceedings of the International Workshop on Numerical Relativity, edited by R. d'Inverno (Cambridge University Press, Cambridge, England, 1992).
[30] H. Friedrich, J. Geom. Phys. **17**, 125 (1995).
[31] H. Friedrich (private communication).
[32] R. Penrose and W. Rindler, *Spinors and Space-Time* (Cambridge University Press, Cambridge, England, 1984), Vols. I, II.